2015

Remote sensing of drought: Progress, challenges and opportunities

A. AghaKouchak
University of California - Irvine, amir.a@uci.edu

A. Farahmand
University of California - Irvine

F. S. Melton
NASA Ames Research Center Cooperative for Research in Earth Science and Technology, forrest.s.melton@nasa.gov

J. Teixeira
NASA Jet Propulsion Laboratory, California Institute of Technology, Pasadena, California

M. C. Anderson
USDA, Agricultural Research Service, martha.anderson@ars.usda.gov

See next page for additional authors

AGU PUBLICATIONS

Reviews of Geophysics

REVIEW ARTICLE
10.1002/2014RG000456

Key Points:
- Current and emerging approaches in satellite remote sensing of drought
- Limitations of currently available satellite observations and challenges ahead
- Opportunities for advancing science of drought remote sensing

Correspondence to:
A. AghaKouchak,
amir.a@uci.edu

Citation:
AghaKouchak, A., A. Farahmand, F. S. Melton, J. Teixeira, M. C. Anderson, B. D. Wardlow, and C. R. Hain (2015), Remote sensing of drought: Progress, challenges and opportunities, *Rev. Geophys.*, *53*, 452–480, doi:10.1002/2014RG000456.

Received 2 APR 2014
Accepted 18 MAY 2015
Accepted article online 23 MAY 2015
Published online 29 Jun 2015

Remote sensing of drought: Progress, challenges and opportunities

A. AghaKouchak[1], A. Farahmand[1], F. S. Melton[2], J. Teixeira[3], M. C. Anderson[4], B. D. Wardlow[5], and C. R. Hain[6]

[1]Center for Hydrometeorology and Remote Sensing, University of California, Irvine, California, USA, [2]NASA Ames Research Center Cooperative for Research in Earth Science and Technology, Moffett Field, California, USA, [3]NASA Jet Propulsion Laboratory, California Institute of Technology, Pasadena, California, USA, [4]United States Department of Agriculture, Agricultural Research Service, Beltsville, Maryland, USA, [5]School of Natural Resources, University of Nebraska-Lincoln, Lincoln, Nebraska, USA, [6]Earth System Science Interdisciplinary Center, University of Maryland, College Park, Maryland, USA

Abstract This review surveys current and emerging drought monitoring approaches using satellite remote sensing observations from climatological and ecosystem perspectives. We argue that satellite observations not currently used for operational drought monitoring, such as near-surface air relative humidity data from the Atmospheric Infrared Sounder mission, provide opportunities to improve early drought warning. Current and future satellite missions offer opportunities to develop composite and multi-indicator drought models. While there are immense opportunities, there are major challenges including data continuity, unquantified uncertainty, sensor changes, and community acceptability. One of the major limitations of many of the currently available satellite observations is their short length of record. A number of relevant satellite missions and sensors (e.g., the Gravity Recovery and Climate Experiment) provide only a decade of data, which may not be sufficient to study droughts from a climate perspective. However, they still provide valuable information about relevant hydrologic and ecological processes linked to this natural hazard. Therefore, there is a need for models and algorithms that combine multiple data sets and/or assimilate satellite observations into model simulations to generate long-term climate data records. Finally, the study identifies a major gap in indicators for describing drought impacts on the carbon and nitrogen cycle, which are fundamental to assessing drought impacts on ecosystems.

1. Introduction

Drought poses significant water and food security concerns, and may lead to economic risks and financial challenges, especially for developing economies [*Wilhite*, 2005; *Godfray et al.*, 2010]. The phenomenon of meteorological drought is a consequence of regional variability in the global water cycle, a process tightly associated with climatic circulation patterns [*Piechota and Dracup*, 1996; *Hidalgo*, 2004; *Rasmusson et al.*, 1983; *Keyantash and Dracup*, 2004; *Golian et al.*, 2014]. For this reason, a global perspective on drought conditions is often necessary to study the cause of specific regional droughts. For example, a recent study links global droughts during the late 1990s and early 2000s to warm and cold sea surface temperatures in the western and eastern tropical Pacific, respectively [*Hoerling and Kumar*, 2003]. Conversely, a regional or continental drought can also lead to global impacts. For example, the 2010 Russian drought and heat wave led to an increase in global food prices [*Wegren*, 2011], resulting in indirect impacts far beyond the drought-affected region. These issues highlight the importance of global, rather than regional, drought monitoring to understanding the biophysical processes involved [*Grasso and Singh*, 2011].

Droughts are broadly classified into four groups including meteorological (deficit in precipitation), agricultural (deficit in soil moisture), hydrological (deficit in runoff, groundwater, or total water storage), and socioeconomic (considering water supply, demand, and social response) droughts [*Wilhite*, 2005]. All types of droughts can be associated with a sustained precipitation deficit. However, different elements of the hydrologic cycle respond to droughts differently.

Historically, droughts have been monitored and investigated using ground-based point observations or interpolated grids [*Hayes et al.*, 1999; *Shen and Tabios*, 1996; *Santos et al.*, 2010; *Aghakouchak et al.*, 2014; *Sheffield et al.*, 2012], primarily from meteorological [*Palmer*, 1965] and agricultural perspectives [*Gallagher et al.*, 1976].

Globally, however, many areas used for agricultural production are not well instrumented (e.g., at least one climate station per 5000 km^2) to provide ground-based observations of precipitation, near-surface air temperature, wind speed, atmospheric water vapor, relative humidity, and atmospheric evaporative demand that are consistent over the long term (i.e., at least 30 years of observation). In many other regions, the available observations are not sufficient to capture the spatiotemporal variability of drought-related variables such as precipitation [*Easterling*, 2013]. Furthermore, observations from different meteorological stations often have different record lengths and variable data quality [*Easterling*, 2013], which makes consistent global drought analysis using ground-based observations challenging [*AghaKouchak and Nakhjiri*, 2012].

Satellite remote sensing of the Earth's weather began in earnest with the Television and Infrared Observation Satellite (TIROS-1) mission in 1960 [*NASA*, 1987]. The success of this mission led to a series of additional weather- and climate-oriented satellite remote sensing missions. Remote sensing satellites can be broadly categorized into two types: geostationary (GEO) and low Earth orbit (LEO) satellites [*Kiladze and Sochilina*, 2003]. GEOs orbit at an altitude of 35,786 km [*McVicar and Körner*, 2013] and their orbits are synchronized with Earth's rotation, allowing them to provide information for a fixed field of view over a portion the Earth's surface. LEOs orbit at altitudes of 200–1200 km [*NASA*, 1995], and are typically placed in Sun-synchronous orbits to obtain more than one observation per day over a given location. Current GEOs carry multispectral radiometers that typically collect information in the visible and infrared (VIS/IR) portion of the electromagnetic spectrum, while LEOs carry a diverse range of sensors, including multispectral and hyperspectral sensors, laser altimeters, microwave (MW) sensors and others. Both GEO and LEO satellite observations have been used extensively for drought monitoring and impact assessment [*Anderson and Kustas*, 2008; *Karnieli et al.*, 2010; *Fensholt et al.*, 2006; *Wang and Qu*, 2007; *McVicar and Jupp*, 1998].

Remote sensing observations have been used to monitor drought-related variables from a climatological viewpoint and also to assess and quantify drought impacts from an ecosystem perspective. In the former, satellite multispectral, thermal infrared, or microwave data are used to retrieve a drought-related variable including precipitation [*Sorooshian et al.*, 2011], soil moisture [*Entekhabi et al.*, 2004; *Cashion et al.*, 2005], or evapotranspiration [*Running et al.*, 1989; *Allen et al.*, 2007; *Anderson et al.*, 2011b; *Price*, 1982]. The specific hydrologic variable is then converted into a drought indicator by calculating the extent of an anomaly or departure from the longer-term environmental baseline. Those data are used to quantitatively assess and categorize drought severity.

Satellite observations have also been used to assess drought ecosystem impacts—including vegetation health and growth—by assessing the photosynthetic capacity of plants [*Tucker and Choudhury*, 1987; *Asner and Alencar*, 2010]. Precipitation deficits can lead to reduced photosynthetic capacity and changes in absorption of solar radiation in photosynthetically active wavelengths by plants [*Asrar et al.*, 1984]. Combinations of satellite visible (VIS) and infrared (IR) images have been widely used to monitor plant changes and water stress [*Asrar et al.*, 1989; *Hatfield et al.*, 1984; *Tucker and Choudhury*, 1987; *Wardlow et al.*, 2012].

In the past decade, the science community has been able to access unprecedented new remote sensing data sets for precipitation, snow, soil moisture, land surface temperature, evaporation, total water storage, vegetation, and land cover [*NASA*, 2010; *Wardlow et al.*, 2012; *Krajewski et al.*, 2006]. These satellite observations have opened new avenues in global drought monitoring from different perspectives (e.g., meteorological, agricultural, hydrological, and ecological). The advantages of satellite-based sensors relative to traditional ground-based observations include global, near-real-time observations, consistent data records, and improved spatial resolution [*Heumann*, 2011; *Barrett et al.*, 1990; *Barrett and Herschy*, 1989; *Morgan*, 1989]. The increasing volume of satellite observations and data products has led the science community into the era of *big data* [*Sellars et al.*, 2013] and provided unique opportunities to develop advanced drought monitoring capabilities using multiple data sources. However, the abundance of data also presents major scientific challenges, including uncertainty assessment, managing data volumes, merging or fusion of multiple data sources, and ensuring consistency between different observations and data sets.

This paper first reviews the progress in remote sensing of drought from climatological and ecosystem perspectives, including satellite-based drought indicators. Then, major research gaps and challenges in advancing remote sensing of drought are discussed. Finally, we outline a path for future research that could lead to a major advance in drought monitoring and impact assessment using space-based observations. This paper focuses only on satellite remote sensing, and not aircraft and airborne remote sensing platforms, since the latter typically have limited geographical and/or temporal coverage.

2. Progress in Remote Sensing of Drought From a Climatological Perspective

In this section, progress in remote sensing of drought-related variables and development of satellite-based drought severity indicators are reviewed.

2.1. Precipitation

A commonly used precipitation-based drought index is the Standardized Precipitation Index (SPI) [*McKee et al.*, 1993], which was recommended by the World Meteorological Organization (WMO) as a global measure of meteorological drought [*WMO*, 2009; *Hayes et al.*, 2011]. Deriving SPI involves describing the frequency distribution of precipitation using either a parametric distribution function [*McKee et al.*, 1993] or a nonparametric approach [*Hao and AghaKouchak*, 2014] for different precipitation accumulation periods (e.g., 1, 3, or 6 month periods). The SPI is computed by transforming the cumulative probability of precipitation into the standard normal distribution. A sequence of negative SPI indicates a dry period, while a sequence of positive values represent a wet spell. In addition to SPI, precipitation percentiles and the Percent of Normal Precipitation (PNP) [*Werick et al.*, 1994] are also used as measures of departure from the climatology and thus, wet/dry conditions.

Several techniques have been developed for routine retrieval of rainfall using satellite data collected in multiple wavebands. Satellite IR and VIS images of cloud top temperature can be converted into a precipitation rate using empirical statistical relationships [*Arkin et al.*, 1994; *Joyce and Arkin*, 1997; *Turk et al.*, 1999]. Passive microwave (MW) sensors offer a more physically based approach to instantaneous precipitation estimation [*Kummerow et al.*, 1996, 2001]. While MW sensors provide more accurate precipitation information, they are limited by their infrequent overpasses ($\approx$ 2 observations per day for any location). GEO IR/VIS data, on the other hand, provide more frequent precipitation information ($\approx$ 15–30 min) although with higher uncertainty [*Sorooshian et al.*, 2011]. Studies suggest that combining both satellite MW and IR information leads to better precipitation estimates, especially of diurnal patterns, by combining the strengths of both sensors [*Joyce et al.*, 2004]. Currently, several satellite precipitation data sets are available including the Climate Predicting Center (CPC) Morphing Technique (CMORPH) [*Joyce et al.*, 2004], Tropical Rainfall Measuring Mission (TRMM) Multi-satellite Precipitation Analysis (TMPA) [*Huffman et al.*, 2007], Precipitation Estimation from Remotely Sensed Information using Artificial Neural Networks (PERSIANN) [*Hsu et al.*, 1997; *Sorooshian et al.*, 2000; *Hong et al.*, 2004], and the Global Precipitation Climatology Project (GPCP) [*Adler et al.*, 2003]—for a comprehensive review of precipitation algorithms see *Levizzani et al.* [2007]and *Kidd* [2001]. These data sets have been extensively intercompared and validated against ground-based observations [*AghaKouchak et al.*, 2012; *Tian et al.*, 2009; *Ebert et al.*, 2007; *Chappell et al.*, 2013; *Nasrollahi et al.*, 2013; *Katiraie-Boroujerdy et al.*, 2013].

Satellite precipitation data sets have been widely used for both model-based and data-driven drought monitoring [*Anderson et al.*, 2008; *Paridal et al.*, 2008; *Damberg and AghaKouchak*, 2014]. The experimental African Drought Monitor integrates satellite observations of precipitation for assessing hydrologic conditions [*Sheffield et al.*, 2006]. One limitation of current near-real-time satellite precipitation products is their short length of record (approximately 15 years). There are a number of products that provide low-resolution long-term records (e.g., GPCP); however, they do not provide real-time observations necessary for operational drought monitoring systems. A near-real-time satellite-based precipitation data set was proposed for operational drought monitoring that combines the near-real-time satellite data with the long-term GPCP observations using a Bayesian data merging model [*AghaKouchak and Nakhjiri*, 2012]. The data set includes SPI based on PERSIANN and TMPA with the climatology obtained from GPCP observations. The Bayesian data merging component makes the data from different sensors/algorithms climatologically consistent for drought monitoring. A sample merged product of GPCP (1979–2009) and PERSIANN (2010 to the present) is presented for July 2010 in Figure 1. The figure shows that the merged product captures the 2010 Russian drought [*Wegren*, 2011], as well as the 2010 Amazon drought [*Lewis et al.*, 2011; *Marengo et al.*, 2011]. Furthermore, the figure highlights the precipitation deficit in East Africa, which led to a major drought during 2010–2011 [*Funk*, 2011]. The main advantage of this data set is that near-real-time satellite data are publicly available within hours to days from the original observations, allowing for near-real-time drought monitoring. Throughout his paper, other remote sensing-based indicators are also shown for the same time step (July 2010) so that the reader can evaluate their similarities and discrepancies.

2.2. Soil Moisture

Soil moisture is a fundamental component of the water cycle and plays a key role in drought monitoring and prediction, especially in water-limited ecosystems [*D'Odorico et al.*, 2007; *Moran et al.*, 2004; *Peters-Lidard et al.*,

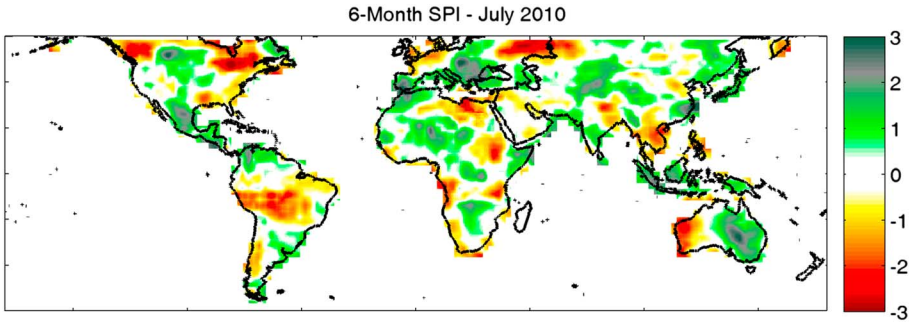

Figure 1. Combining different remote sensing data sets (here GPCP and PERSIANN) for global near-real-time drought monitoring using Standardized Precipitation Index (SPI)-July 2010.

2008]. Soil moisture is often used as a measure of agricultural drought since it affects plant growth and productivity [*Boken et al.*, 2005; *Wilhite*, 2005]. A number of soil moisture-based indices have been developed and used for drought monitoring, including the Standardized Soil Moisture Index (SSI) [*Hao and AghaKouchak*, 2013] and the soil moisture percentile [*Sheffield et al.*, 2004; *Wang et al.*, 2009]. Soil moisture is a particularly important variable for monitoring drought persistence and development [*AghaKouchak*, 2014a]. The soil moisture input to these drought indicators can be obtained from land surface model simulations or from satellite estimates.

Most satellite soil moisture algorithms are based on passive MW [*Njoku et al.*, 2003; *Jackson*, 1997; *Njoku and Entekhabi*, 1996], active MW [*Wagner et al.*, 1999; *Takada et al.*, 2009], or a blend of data from multiple sensors [*Wilson et al.*, 2001; *Gruhier et al.*, 2010; *Entekhabi et al.*, 2010a; *Liu et al.*, 2011a; *Kim and Hogue*, 2012]. The principal of MW-based soil moisture retrieval relies on the relationship between soil permittivity and liquid water content. There are empirical relationships that link passive MW brightness temperature and active MW backscattering to volumetric water content of soil. MW soil moisture observations typically represent the top 2–5 cm of soil depth [*Entekhabi et al.*, 2010a; *Njoku et al.*, 2003; *Wang and Qu*, 2009]. For root-zone soil surface moisture estimates, MW soil moisture observations can be coupled to an appropriate land surface model [*Reichle et al.*, 2004]. For a comprehensive review of optical, thermal, passive MW, and active MW soil moisture monitoring approaches, see *Wang and Qu* [2009].

The long-term satellite-based soil moisture time series obtained from the Water Cycle Multi-Mission Observation Strategy (WACMOS) have been used for drought detection and monitoring in the Horn of Africa region [*Ambaw*, 2013]. The United States Department of Agriculture (USDA) International Production Assessment Division (IPAD) estimates surface and root-zone soil moisture with a two-layer modified Palmer soil moisture model forced by global precipitation and near-surface air temperature measurements [*Palmer and Havens*, 1958]. In this approach, only near-surface air temperature is used to approximate potential evapotranspiration, which has limitations when estimating evapotranspiration [*McVicar et al.*, 2012; *Donohue et al.*, 2010; *Hobbins et al.*, 2008]. Soil moisture data retrieved from the Advanced Microwave Scanning Radiometer–Earth Observing System (AMSR-E) [*Jackson*, 1993] have been integrated into the real-time USDA IPAD soil model to improve drought monitoring and prediction [*Bolten et al.*, 2010].

Recently, the Climate Change Initiative (CCI) for Soil Moisture began offering global satellite-based soil moisture data derived from multiple sensors [*Wagner et al.*, 2012; *Liu et al.*, 2011a]. As the CCI Soil Moisture data set is over 30 years long, it can be used for monitoring agricultural drought, and monthly or seasonal changes in soil moisture patterns within a much longer historical context than most remote sensing-based data products derived from a single sensor or satellite mission (see Figure 2). The CCI soil moisture data have gaps, mainly over densely vegetated land areas, even at monthly scales (see the Amazon and central Africa in Figure 2). However, there are opportunities to assimilate data sets like CCI into land surface models, or to apply satellite-derived data sets for calibration of land surface model parameters to generate long-term, consistent soil moisture fields [*Reichle et al.*, 2004]. It is also noted that the spatial patterns in the CCI soil moisture and satellite precipitation data are generally consistent, even though they are sampling different components of the hydrologic budget (e.g., compare Australia and Russia in Figures 1 and 2). The CCI soil moisture data are yet to be fully explored for global drought monitoring and assessment, and it is anticipated that future studies on global trends and patterns of droughts will use this data set.

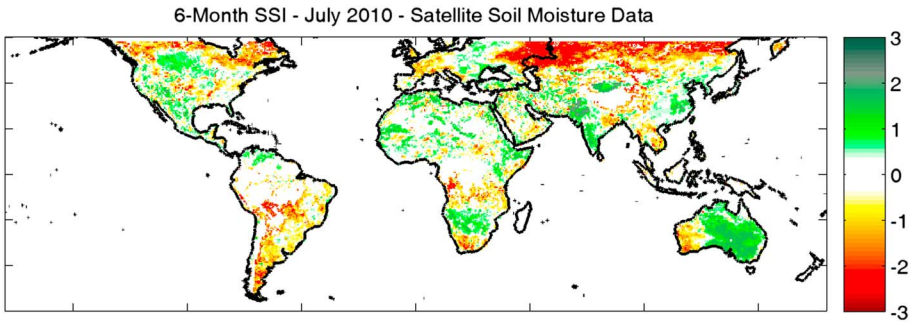

Figure 2. Standardized Soil Moisture (SSI) based on CCI satellite soil moisture observations-July 2010.

2.3. Groundwater and Terrestrial Water Storage

Estimates of drought impacts on terrestrial water storage and groundwater conditions at regional to global scales can be obtained using the Gravity Recovery and Climate Experiment (GRACE) mission. GRACE responds to all factors that change the gravity field of an area, including the terrestrial water storage (TWS). Launched in 2002, the GRACE mission tracks global variations in gravity fields that can be converted into estimates of TWS [*Rodell and Famiglietti*, 2002]. The principle of gravimetry and TWS estimation is that bulk surface and subsurface water mass has a gravitational potential that alters the Earth's gravity field, allowing changes in the Earth's gravitational field to be used as an indicator of changes in the total amount of water stored in the vertical continuum. GRACE consists of two identical satellites separated by a distance of about 220 km that orbit the Earth at an altitude of approximately 500 km. Changes in the Earth's gravity fields alter the distance between the two spacecraft. Having accurate measures of the distance between the two spacecraft, one can quantify temporal TWS anomalies, which include the sum of surface water, groundwater, soil moisture, snow/ice, and moisture stored in vegetation [*Rodell*, 2012].

Having TWS, changes to groundwater ΔG can be approximated as $\Delta G = \Delta\mathrm{TWS} - \Delta\mathrm{SM} - \Delta\mathrm{SWE}$, where SM and SWE represent soil moisture and snow water equivalent, respectively [*Rodell et al.*, 2007]. GRACE-based TWS data have been widely used for drought monitoring and water storage assessment over numerous areas including the Canadian Prairie [*Yirdaw et al.*, 2008], Australia [*Leblanc et al.*, 2009; *van Dijk et al.*, 2011, 2013], the Amazon River basin [*Chen et al.*, 2009], and western and central Europe [*Li et al.*, 2012]. During the 2011 Texas drought, the TWS data set was found to be a valuable tool for monitoring statewide water storage depletion, and for linking meteorological and hydrological drought conditions [*Long et al.*, 2013].

Currently, GRACE provides 12 years of data, which may not be sufficient for climatological drought assessment. An additional limitation of GRACE data for regional drought assessments has been the spatial resolution of >150,000 km^2 per pixel for GRACE TWS data [*Houborg et al.*, 2012]. Recently, GRACE data have been downscaled to higher resolutions via assimilation into land surface models [*Zaitchik et al.*, 2008]. This approach offers potential for improved drought monitoring and assessment of associated reductions in groundwater supplies at finer spatial scales. Using the GRACE data assimilation system (GRACE-DAS) [*Zaitchik et al.*, 2008] and the Catchment land surface model (CLSM) [*Koster et al.*, 2000], a GRACE-based drought indicator has been developed and integrated into the United States and North America Drought Monitor [*Houborg et al.*, 2012]. Given that GRACE offers information on the total water storage deficit [*Thomas et al.*, 2014], it can be used to estimate the amount of water (precipitation) needed to recover from drought events.

2.4. Evapotranspiration

Evapotranspiration (ET) is an important component of the water and energy cycle, reflecting mass and energy exchange between ecosystems and the atmosphere [*Senay et al.*, 2012; *Wang and Dickinson*, 2012]. Atmospheric evaporative demand is a function of net radiation, air temperature, wind speed, and relative humidity [*Donohue et al.*, 2010; *Hobbins et al.*, 2008; *McVicar et al.*, 2012; *Yin et al.*, 2014]. While ground-based measurement of ET at large spatial extents is challenging, remote sensing data sets offer a unique opportunity to provide large-scale estimates of ET. A unique feature of ET for drought monitoring is that it describes both water/moisture availability and the rate at which it is consumed [*M. C. Anderson et al.*, 2012]. Broadly, remote sensing-based ET estimation methods can be categorized into the following groups based on (a) principles of water balance [*Allen et al.*, 1998; *Senay*, 2008], (b) principles of surface energy balance [*Allen et al.*, 2007; *Anderson and Kustas*, 2008; *Senay et al.*, 2007; *Kalma et al.*, 2008; *Su et al.*, 2005], (c) vegetation indices [*Glenn*

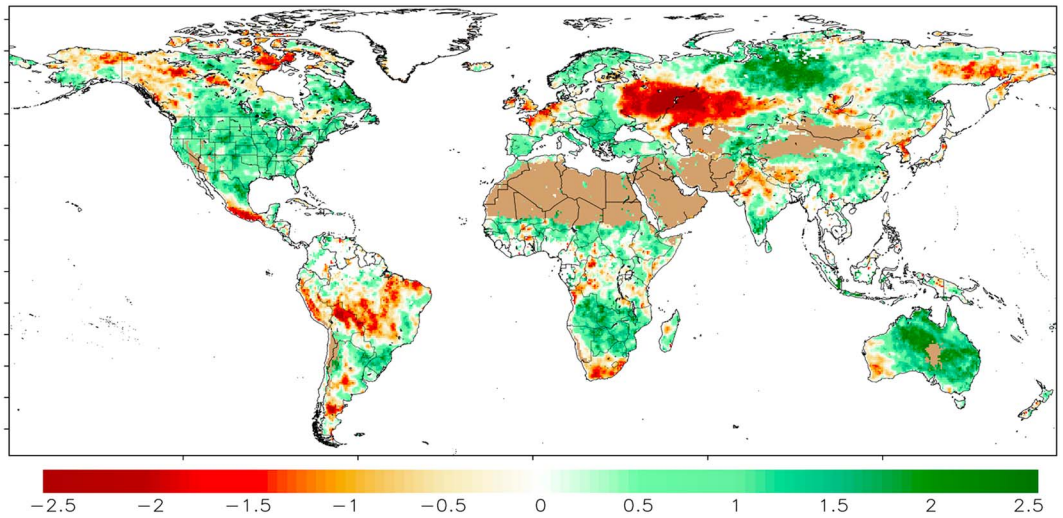

Figure 3. Evaporative Stress Index (ESI) for July 2010, expressed as standardized anomalies. Red indicates lower than normal AET/PET or depressed rates of relative water use. Regions where ET is persistently low and standardized anomalies cannot be reliably determined are shown in brown.

et al., 2011; *Yebra et al.*, 2013], and (d) hybrid approaches based on vegetation indices and surface temperature information [*Carlson*, 2007; *Yang and Shang*, 2013; *Kalma et al.*, 2008]. Water balance models track changes in moisture in the soil for ET estimation, whereas energy balance models use land surface temperature (LST) and meteorological data to estimate sensible heat flux and moisture/water fluxes [*Kalma et al.*, 2008; *Norman et al.*, 1995; *Morillas et al.*, 2013; *Glenn et al.*, 2007].

Several drought indicators have been developed that integrate ET as an input variable such as the Crop Water Stress Index (CWSI) [*Idso et al.*, 1981; *Jackson et al.*, 1981], Water Deficit Index (WDI) [*Moran et al.*, 1994], Evaporative Stress Index (ESI) [*Anderson et al.*, 2011a, 2013a], Evaporative Drought Index (EDI) [*Yao et al.*, 2010], Drought Severity Index (DSI) [*Mu et al.*, 2013], and Reconnaissance Drought Index (RDI) [*Tsakiris and Vangelis*, 2005; *Tsakiris et al.*, 2007].

The CWSI is based on the ratio of the actual ET (AET) to potential ET (PET) and is expressed as CWSI = 1 − AET/PET. The WDI, follows the same concept, but is based on the AET rate (λ_{AET}) and PET rate (λ_{PET}): WDI = 1 − $\lambda_{AET}/\lambda_{PET}$. The ESI is defined as the standardized anomalies in the ratio of AET to PET [*Anderson et al.*, 2011b]. In this approach, the ET estimation is based on thermal infrared remote sensing data and the Atmosphere-Land Exchange Inverse (ALEXI) model [*Anderson et al.*, 1997; *Mecikalski et al.*, 1999; *Anderson et al.*, 2007]. Figure 3 shows the ALEXI-based Evaporative Stress Index (ESI) for July 2010, derived using Moderate Resolution Imaging Spectroradiometer (MODIS) day-night land surface temperature differences. ESI clearly shows deficits in actual evapotranspiration associated with drought conditions particularly over Russia and central Asia, Brazil, South Africa, and southwestern Australia. Evaluation studies indicate that ESI is a promising drought indicator for characterizing streamflow and soil moisture anomalies [*Choi et al.*, 2013] and provides valuable information for early warning of rapidly developing drought conditions, often referred to as "flash" droughts [*Anderson et al.*, 2013b; *Otkin et al.*, 2014]. Similar to ESI, EDI is based on AET and PET (EDI = 1 − AET/PET) and has been used to monitor drought at continental and global scales [*Yao et al.*, 2011].

The DSI is defined as the summation of the normalized ratio of AET/PET and the normalized difference vegetation index (NDVI) [*Mu et al.*, 2013]. In this approach, the ratio of AET/PET is derived using shortwave satellite observations from the Moderate Resolution Imaging Spectroradiometer (MODIS) within a Penman-Monteith ET formulation [*Mu et al.*, 2007, 2009, 2011]. Results indicate that the DSI is consistent with both precipitation-based drought indices as well as satellite-based measures of vegetation net primary production (NPP) [*Running et al.*, 2004]. Unlike most drought indices, DSI is not a standardized measure of drought severity, but rather a dimensional index ranging from $[-\infty, \infty]$, where a lower index value indicates a more severe drought condition.

The RDI is defined as the ratio of the aggregated precipitation (P) and PET and has been widely used in the literature for drought monitoring [e.g., *Tsakiris and Vangelis*, 2005; *Tsakiris et al.*, 2007]. The P/PET ratio is also

termed as the aridity index [*UNESCO*, 1979] and can be standardized for cross comparison with other drought indicators. The RDI is different from the other indices in the sense that it does not use AET. The RDI has been used with PET estimates derived from satellite-retrieved air temperature data [*Dalezios et al.*, 2012]. However, this is a simplistic assumption as other key meteorological variables including net radiation, wind speed, and relative humidity affect PET rates [*McVicar et al.*, 2012; *Donohue et al.*, 2010].

2.5. Snow

Snow is considered a natural reservoir of water resources, and in some regions snow melt constitutes a substantial fraction of the annual runoff [*Kongoli et al.*, 2012; *Bales et al.*, 2006]. A deficit in the winter snowpack could potentially lead to a summer hydrological drought (e.g., reduced stream flows and/or groundwater levels) or agricultural drought (e.g., depleted soil moisture reserves to support plant functions), and hence, monitoring snow is fundamental to drought assessment in many regions. From a hydrological viewpoint, the drought-relevant snow parameters include the following: snow water equivalent (SWE), snow-covered area (SCA), snow depth (SD), and snow albedo (SA) [*Kongoli et al.*, 2012; *Painter et al.*, 2013; *Molotch and Bales*, 2006]. Remotely sensed snow estimation methods can be broadly categorized into three groups: (a) optical, (b) MW, and (c) composite optical and MW. Optical-based products provide estimates of only SCA, whereas MW-based and composite products provide information on SCA, SD, and SWE.

The basis of optical snow monitoring relies on the fact that snow exhibits a strong spectral gradient in reflectance, from high albedo in visible wavelengths to low reflectance in middle IR wavelengths [*Dozier et al.*, 2009; *Kongoli et al.*, 2012; *Wiscombe and Warren*, 1980]. Thus, snow can be monitored using the ratio of the visible reflectance (R_{VIS}) and the middle IR reflectance (R_{mIR}) [*Romanov et al.*, 2000]. Alternatively, snow can be detected using the Normalized Difference Snow Index (NDSI) defined as $(R_{\mathrm{VIS}} - R_{\mathrm{mIR}})/(R_{\mathrm{VIS}} + R_{\mathrm{mIR}})$ [*Hall et al.*, 2002]. A suite of optical-based snow products are available from MODIS with a wide range of temporal and spatial resolutions [*Hall et al.*, 2002]. A number of snow algorithms have also been developed based on the advanced very high resolution radiometer (AVHRR) satellite data record [*Simpson et al.*, 1998]. However, the accuracy of optical-based snow estimates can be compromised by clouds that exhibit similar spectral features [*Kongoli et al.*, 2012; *Bromwich et al.*, 2012]. Furthermore, persistent cloud cover can hinder temporally continuous snow monitoring.

Microwave radiation, on the other hand, penetrates through clouds and provides a unique opportunity for temporally continuous snow monitoring [*Kongoli et al.*, 2012; *Schanda et al.*, 1983]. More importantly, microwaves can penetrate into snow, allowing estimation of SWE and SD that cannot be obtained from optical-based methods [*Durand et al.*, 2008]. A number of algorithms have been developed for estimation of SCA using microwave data sets [*Grody and Basist*, 1996]. Microwave-based estimates of SWE and SD are mainly based on an empirical regression between variations in observed SWE and SD and the difference in brightness temperature in two low-frequency channels [*Kongoli et al.*, 2007]. There are static empirical algorithms in which one set of regression parameters are used [*Kunzi et al.*, 1982; *Goodison*, 1989], as well as dynamic empirical algorithms in which different regression coefficients are used in various regions and for different seasons [*Foster et al.*, 2005; *Kelly et al.*, 2003].

Currently, microwave sensors are only available onboard polar-orbiting satellites that have longer revisit times relative to optical sensors onboard geostationary satellites. For this reason, the temporal frequency of microwave-based snow estimates is typically lower than those of the optical-based products. Recently, snow retrieval algorithms have been developed based on merged optical and microwave data sets to address limitations of individual sensors [*Foster et al.*, 2011; *Liang et al.*, 2008; *Durand et al.*, 2008].

Remotely sensed and in situ snow information has been used in a number of drought studies [*Wiesnet*, 1981; *Kongoli et al.*, 2012; *Painter et al.*, 2013; *Guan et al.*, 2013; *Molotch and Margulis*, 2008]. Most studies focus on assimilating satellite snow information into land surface or hydrological models to improve streamflow simulation and hence, hydrological drought prediction [*Dong et al.*, 2007; *Andreadis and Lettenmaier*, 2005; *Margulis et al.*, 2006; *He et al.*, 2012]. Unlike other drought-related variables, snow-based indicators of drought are still in their infancy, primarily because there is a lag between snow occurrence and change in surface water and soil moisture availability that varies in space and time. Runoff from snowmelt could affect water availability on timescales from a few weeks (e.g., low-elevation snow and in lower latitudes) or a few months (e.g., high-elevation snow and in higher latitudes). This lag time is a significant strength for drought early warning. However, even over one particular location, depending on seasonal temperatures and the timing of snow

accumulation, the lag time from snowfall, snowmelt, and runoff varies substantially. This highly variable lag is the main challenge in deriving snow-based indicators for drought monitoring.

3. Progress in Remote Sensing of Drought From an Ecological Perspective

Drought can be assessed based on observed changes in vegetation health and land cover from remotely sensed data [*Tucker and Choudhury*, 1987; *Silleos et al.*, 2006; *Nemani et al.*, 2009]. The launch of the first AVHRR instrument in 1979 transformed remote sensing of drought by providing high temporal resolution data for systematic monitoring of vegetation patterns and conditions. Quantitative assessment of vegetation condition is generally based on the spectral signature of vegetation greenness expressed in the red (R) and near-infrared (NIR) portions of the electromagnetic spectrum [*Boken et al.*, 2005].

The normalized difference vegetation index (NDVI) [*Rouse et al.*, 1974] is the most frequently used vegetation index [*Tucker*, 1979; *Karnieli et al.*, 2010; *Funk and Budde*, 2009] and the first remote sensing-based measure used to monitor agricultural drought. NDVI is the difference between reflected R and NIR radiation divided by the their sum [*Rouse et al.*, 1974]: $(\mathrm{NDVI} = (\rho_{\mathrm{NIR}} - \rho_{\mathrm{R}})/(\rho_{\mathrm{NIR}} + \rho_{\mathrm{R}}))$. Since the soil spectrum and nonvegetated surfaces do not exhibit distinct differences in spectral absorption between the R and NIR bands, NDVI can be used to separate vegetation from the soil background [*Karnieli et al.*, 2010] and provide a measure of general vegetation health. Time series decomposition [*Donohue et al.*, 2009; *Lu et al.*, 2003] provides the means to assess persistent and recurrent vegetation conditions, which may be related to deep-root or shallow-rooted vegetation types in ecosystems.

A significant relationship has been reported between NDVI and precipitation and soil moisture [*Di et al.*, 1994; *Farrar et al.*, 1994; *Adegoke and Carleton*, 2002; *Hielkema et al.*, 1986; *Richard and Poccard*, 1998; *Wang et al.*, 2001], and thus, NDVI (or its derivatives) has been widely used for drought assessment and vegetation health monitoring [*Tucker and Choudhury*, 1987; *Prince et al.*, 1998; *Nicholson et al.*, 1998; *Ji and Peters*, 2003; *McVicar and Jupp*, 1998]. The general vegetation health can be temporally decomposed to monitor changes in recurrent (shallow-rooted) and persistent (deeper-rooted) vegetation for many landscapes across the globe [*Donohue et al.*, 2009; *Lu et al.*, 2003; *Roderick et al.*, 1999]. This is particularly important when monitoring drought in savannahs or areas with mixed trees and ecosystems across semiarid regions [*Donohue et al.*, 2009].

Building on the original definition of NDVI, a number of other indicators have been developed such as the Transformed Vegetation Index (TVI) [*Deering and Rouse*, 1975; *Tucker*, 1979], Perpendicular Vegetation Index (PVI) [*Wiegand et al.*, 1991], Corrected Transformed Vegetation Index (CTVI) [*Perry and Lautenschlager*, 1984], and Thiam's Transformed Vegetation Index (TTVI) [*Thiam*, 2013]—see *Silleos et al.* [2006] and *Payero et al.* [2004] for a comprehensive list. These indices describe the vegetation condition by combining spectral information from different parts of the electromagnetic spectrum that are sensitive to biophysical characteristics of vegetation, such as chlorophyll content, water content, and internal leaf structure.

The Vegetation Condition Index $(\mathrm{VCI} = (\mathrm{NDVI} - \mathrm{NDVI}_{\mathrm{min}})/(\mathrm{NDVI}_{\mathrm{max}} + \mathrm{NDVI}_{\mathrm{min}}))$, for example, scales NDVI values between its minimum and maximum values to separate the short-term weather signal from the long-term ecological signal for drought monitoring [*Kogan and Sullivan*, 1993], and it has been used for monitoring drought and phenological change in several studies [*Kogan*, 1997; *Liu and Kogan*, 1996; *Quiring and Ganesh*, 2010; *Singh et al.*, 2003; *McVicar and Jupp*, 1998]—Figure 4. Use of the monthly VCI is more appropriate in areas with a large land management signal (e.g., cropping) and hence is suitable for monitoring agricultural drought [*McVicar and Jupp*, 1998]. A standardized form of NDVI, known as the Standardized Vegetation Index (SVI), is based on the *z* score of NDVI values [*Peters et al.*, 2002; *Park et al.*, 2008]: $\mathrm{SVI} = (\mathrm{NDVI}_{ijk} - \overline{\mathrm{NDVI}}_{ij})/\sigma_{ij}$. The SVI is computed for each pixel (i), week (j), and year (k). The terms $\overline{\mathrm{NDVI}}_{ij}$ and σ_{ij} denote the mean and standard deviation of the pixel (i) over $k = 1, \ldots, n$ years.

There are other indices based on R and NIR bands such as the Normalized Ratio Vegetation Index (NRVI) [*Baret and Guyot*, 1991], Soil-Adjusted Vegetation Index (SAVI) [*Huete*, 1988], Perpendicular Drought Index (PDI) [*Ghulam et al.*, 2007a], Modified Perpendicular Drought Index (MPDI) [*Ghulam et al.*, 2007b], Distance Drought Index (DDI) [*Qin et al.*, 2010], and Enhanced Vegetation Index (EVI) [*Huete et al.*, 2002]. The latter, for example, improves sensitivity over high biomass regions and reduces the soil background effects and atmospheric influence [*Justice et al.*, 2002; *Silleos et al.*, 2006; *Huete et al.*, 1999]. A recent study shows that the vegetation water indices outperform the vegetation greenness indices, including the EVI, in high biomass ecosystems [*Caccamo et al.*, 2011]. More specifically, the normalized difference infrared index using MODIS

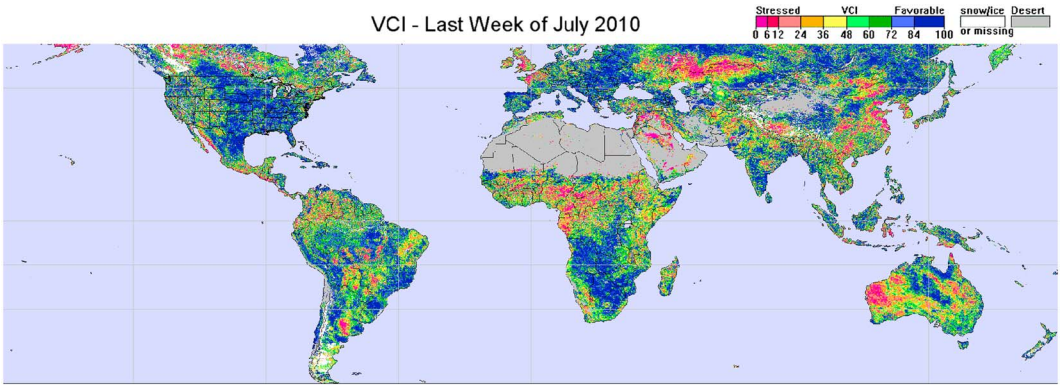

Figure 4. Vegetation Condition Index (VCI) for the last week of July 2010 (source: NOAA/NIDIS Global Vegetation Health data, http://www.star.nesdis.noaa.gov/smcd/emb/vci/VH/index.php).

band 6 (NDIIb6), MODIS band 7 (NDIIb7) [*Hunt and Rock*, 1989], and the D1640 [*Van Niel et al.*, 2003] (Depth of MODIS band 6 (1640 nm) relative to the response between MODIS band 7 (2130 nm) and band 5 (1240 nm)) provides better agreement with precipitation, indicating that in high biomass environments variations in vegetation water content are more dynamic than changes in vegetation greenness properties [*Van Niel et al.*, 2003; *Caccamo et al.*, 2011].

Drought stress can also be quantified using remotely sensed surface brightness temperature derived from thermal channels from multiple satellite instruments (e.g., AVHRR, MODIS, VIIRS, TM, ETM+, and TIRS). The land surface temperature (LST) computed from thermal infrared (TIR) bands has been found to provide valuable information on surface moisture conditions [*Gutman*, 1990]. The Temperature Condition Index (TCI) is based on TIR observations to determine temperature-related vegetation stress. The TCI is defined as TCI $=$ $100(B_{max}-B)/(B_{max}-B_{min})$, where B, B_{max}, and B_{min} denote the smoothed weekly temperature and its multiyear maximum and minimum, respectively [*Kogan*, 1995]. Using data from instruments such as AVHRR and MODIS, TCI may be computed at weekly time scales. An example of TCI for the last week of July 2010 is presented in Figure 5, which is consistent with drought information based on precipitation and soil moisture (Figures 1 and 2). One limitation of TCI is that it does not account for day of year and/or time of day, since it only relies on smoothed weekly temperatures and their multiyear maxima and minima. This issue has been addressed in the development of the normalized difference temperature index (NDTI) [*McVicar and Jupp*, 1999, 2002] that can be considered a specific time-of-day version of the CWSI [*McVicar and Jupp*, 2002].

Studies show that TCI coupled with VCI provides a powerful tool for monitoring vegetation stress and drought condition [*Singh et al.*, 2003], and the two indices have been widely used over different regions [*Unganai and Kogan*, 1998; *Jain et al.*, 2009]. The reflective-based and thermal-based information have been combined for effective and integrated (vegetation temperature) drought information using a combination of the reflective and thermal channels (e.g., combination of NDVI and LST) [*McVicar and Jupp*, 1998; *Karnieli et al.*, 2010;

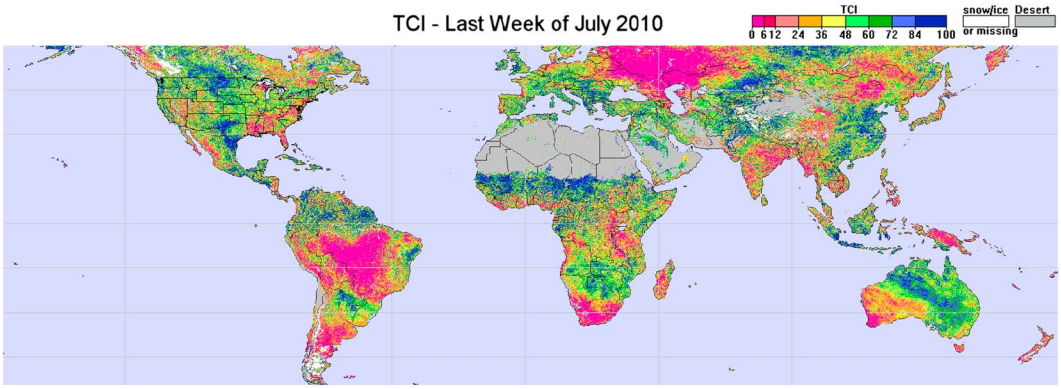

Figure 5. Temperature Condition Index (TCI) for the last week of July 2010 (source: NOAA/NIDIS Global Vegetation Health data).

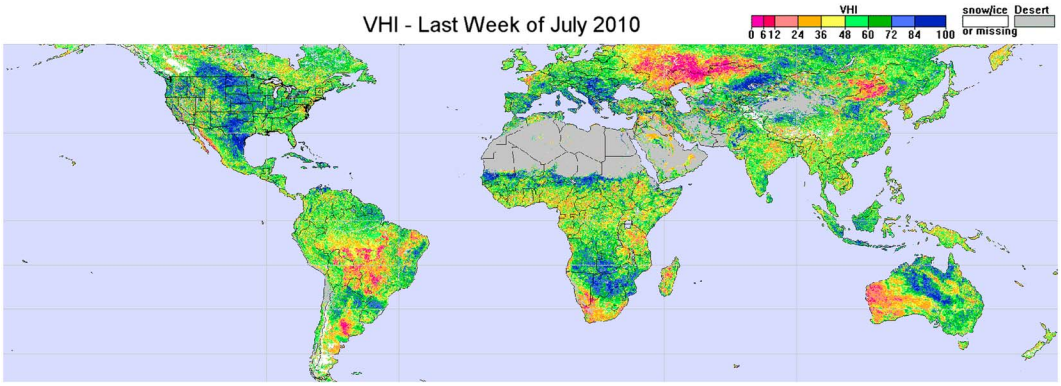

Figure 6. Vegetation Health Index (VHI) for the last week of July 2010 (source: NOAA/NIDIS Global Vegetation Health data).

Bayarjargal et al., 2006]. The Vegetation Temperature Condition Index (VTCI) [*Wan et al.*, 2004] integrates NDVI, LST and thermal properties and provides one index that reflects drought information based on both temperature and vegetation [*Patel et al.*, 2012]. The vegetation health index (VHI) is among the commonly used reflective-thermal indicators that integrates the VCI and TCI [*Kogan*, 1995]: $\mathrm{VHI} = \alpha\mathrm{VCI} + (1-\alpha)\mathrm{TCI}$, where α refers to the relative contribution of the VCI and TCI. Similar to the VCI and TCI, the VHI is typically computed on a weekly time scale and has been used for both drought detection and early warning in different regions [*Seiler et al.*, 1998; *Kogan*, 2001]. An example of VHI is provided in Figure 6, which essentially combines information from Figures 4 and 5.

In recent years, various ways of combining NDVI and LST information have been explored for drought monitoring and impact assessment [*Swain et al.*, 2011; *Son et al.*, 2012]. Such methods rely on the relationship (typically, negative correlation) between LST and NDVI [*Lambin and Ehrlich*, 1996; *McVicar and Bierwirth*, 2001; *McVicar and Jupp*, 1998; *Karnieli et al.*, 2010]. The relationship between the LST and NDVI depends on the season of year and time of day [*Sun and Kafatos*, 2007; *McVicar and Jupp*, 1999, 2002]. Furthermore, the LST-NDVI relationship is associated with moisture condition and climatic/radiation regimes [*Karnieli et al.*, 2010]. A comprehensive study of LST-NDVI relationship over the North American continent and during the summer growing season (April–September) showed that the LST-NDVI correlation is negative when water is the limiting factor for vegetation growth, while the correlation is positive when solar radiation is the limiting factor for vegetation growth [*Karnieli et al.*, 2010]. It is recommended to restrict the use of empirical LST-NDVI relationships for drought monitoring to regions and periods with negative correlation between LST and NDVI (i.e., where water is the primary limiting factor [*Karnieli et al.*, 2010]).

A number of vegetation stress and drought indicators have been developed using shortwave infrared (SWIR) data such as the Normalized Difference Water Index (NDWI) [*Gao*, 1996; *Gu et al.*, 2008, 2007]. The NDWI is defined as the difference between two SWIR bands (typically, 0.86 nm and 1.24 nm) divided by their sum ($\mathrm{NDWI} = (\rho_{0.86\mu m} - \rho_{1.24\mu m})/(\rho_{0.86\mu m} + \rho_{1.24\mu m})$). These two channels sense similar depth through the vegetation canopy and are less sensitive to atmospheric scattering effects than NDVI. Other SWIR bands (e.g., 1.55 μm, 1750 μm, 0.64 μm, 2.13 μm) have been also employed for deriving NDWI using data from the Landsat thematic mapper (TM) onboard Landsat 5, and the Enhanced Thematic Mapper (ETM) onboard Landsat 7 [*Jackson et al.*, 2004; *Chen et al.*, 2005; *Wang and Qu*, 2009].

Sensitivity of NDWI and NDVI to drought conditions has been explored and different results have been reported [*Gu et al.*, 2007, 2008]. To combine information from NDVI and NDWI, the Normalized Difference Drought Index (NDDI) has been proposed as: $\mathrm{NDDI} = (\mathrm{NDVI} - \mathrm{NDWI})/(\mathrm{NDVI} + \mathrm{NDWI})$ [*Gu et al.*, 2007]. It is should be noted that SWIR bands respond to soil moisture and leaf water content differently and, thus, combining multiple SWIR bands (rather than one SWIR band) with a NIR band may improve sensitivity for drought monitoring [*Wang et al.*, 2008]. To address this issue, the Normalized Multi-band Drought Index (NMDI) has been proposed for monitoring soil and vegetation moisture condition using Moderate Resolution Imaging Spectroradiometer (MODIS) data [*Wang and Qu*, 2007]: $\mathrm{NMDI} = (\rho_{0.86\mu m} - (\rho_{1.64\mu m} - \rho_{2.13\mu m}))/(\rho_{0.86\mu m} + (\rho_{1.64\mu m} - \rho_{2.13\mu m}))$. In NMDI, the 0.86 μm band is NIR, whereas the 1.64 μm and 2.13 μm are SWIR bands. By combining information from different channels, the NMDI enhances the sensitivity to drought severity [*Wang*

and Qu, 2007]. Similar efforts have focused on combining Visible data with SWIR information which led to the development of the Visible and Shortwave infrared Drought Index [*Zhang et al.*, 2013]. This indicator combines MODIS blue (band 3), red (band 1), and SWIR (band 6) information.

4. Composite and Multi-Index Drought Models

Several studies argue that drought monitoring efforts should be based on multiple variables/indicators [*Hao and AghaKouchak*, 2013; *Keyantash and Dracup*, 2004; *Kao and Govindaraju*, 2010; *Hao and Singh*, 2015] to provide a more robust and integrated measure of drought that captures the diverse range of vegetation response to drought across different ecosystems. The Vegetation Drought Response Index (VegDRI) [*Tadesse et al.*, 2005; *Brown et al.*, 2008] integrates climate-based drought indices, satellite-based observations of vegetation conditions, and other biophysical information (e.g., land cover type, soil characteristics, and elevation) to describe the levels of vegetation drought stress. The model concept of VegDRI builds upon NDVI [*Rouse et al.*, 1974]. While NDVI is proven to provide valuable information on vegetation health, one may not be able to identify the root causes of vegetation stress solely from NDVI [*Heim*, 2002]. The main reason is that many factors such as fire, land cover change, plant disease, pest infestation, biomass harvesting, and flooding can cause anomalies in NDVI similar to those caused by drought. To address this limitation, VegDRI incorporates climate-based data from SPI and the Palmer Drought Severity Index (PDSI) [*Palmer*, 1968] as additional indicators of dryness and analyzes them in combination with satellite-based NDVI information [*Brown et al.*, 2008].

In a recent study, a triple collocation analysis (TCA) of different soil moisture products (i.e., microwave Advanced Microwave Scanning RadiometerŰ-EOS (AMSR-E), thermal remote sensing using ALEXI, and physically based model simulations) has been suggested for composite drought monitoring [*W. B. Anderson et al.*, 2012]. The final composite soil moisture product takes advantage of the strength of each approach. The approach was validated for the 2010–2011 Horn of Africa drought and has shown promising results for drought monitoring [*W. B. Anderson et al.*, 2012].

An alternative composite model is the Microwave Integrated Drought Index (MIDI) [*Zhang and Jia*, 2013], designed for monitoring short-term drought, especially meteorological drought over semiarid regions. The MIDI integrates satellite-based precipitation data from the Tropical Rainfall Measuring Mission (TRMM) and soil moisture and land surface temperature data from the Advanced Microwave Scanning Radiometer–EOS (AMSR-E): $\mathrm{MIDI} = \alpha\mathrm{PCI} + \beta\mathrm{SMCI} + (1-\alpha-\beta)\mathrm{TCI}$, where PCI is the Precipitation Condition Index, SMCI is the Soil Moisture Condition Index, and TCI is the Temperature Condition Index. Based on the same concept, additional indices can be obtained based on two variables (e.g., $\alpha\mathrm{PCI} + (1-\alpha)\mathrm{SMCI}$). A similar concept is used in the Scaled Drought Condition Index (SDCI) [*Rhee et al.*, 2010], which is a multisensor indicator designed for agricultural drought monitoring in both arid/semiarid and humid regions. The SDCI combines TRMM-based precipitation data, with LST and NDVI information (all three scaled from 0 to 1) for composite drought assessment: $\mathrm{SDCI} = \alpha\mathrm{LST} + \beta\mathrm{TRMM} + \gamma\mathrm{NDVI}$, where $\alpha + \beta + \gamma = 1$. Evaluation of SDCI has shown that the SDCI outperformed the VHI and NDVI over both arid (Arizona and New Mexico) and humid/subhumid (North Carolina and South Carolina) regions [*Rhee et al.*, 2010]. It should be noted that using multiple indicator for composite drought assessment is only useful if the selected indicators provide information that is not fully correlated with each other.

There are also composite approaches that combine physically based model simulations and satellite observations for drought monitoring. For example, the United States Drought Monitor (USDM) [*Svoboda et al.*, 2002] provides weekly drought monitoring information based on a composite of indicators from satellite observations (e.g., VegDRI, VHI, ESI, and GRACE TWS), in situ measurements, and guidance from experts on the ground. The final product collectively analyzes all of this information, which is fused into a single USDM map of drought conditions relying on expertise from climatologists from across the United States.

Finally, the Global Integrated Drought Monitoring and Prediction System (GIDMaPS) [*Hao et al.*, 2014] provides composite drought information based on the Multivariate Standardized Drought Index (MSDI) [*Hao and AghaKouchak*, 2014]. The MSDI has been developed for multi-index drought assessment using precipitation and soil moisture and has been used in a number of drought studies [*AghaKouchak*, 2014b; *Hao and AghaKouchak*, 2013]. A unique feature of MSDI is that it combines meteorological and agricultural drought information into a composite assessment. Different data sets, including satellite observations and model simulations, can be used as inputs to obtain a composite drought map (see an example in Figure 7 based on global precipitation and soil moisture data). This model is standardized, and thus provides drought

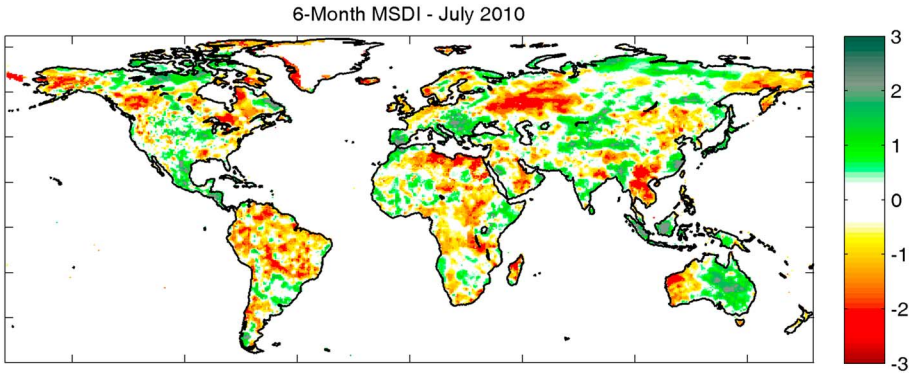

Figure 7. Multivariate Standardized Drought Index (MSDI) for July 2010, derived from the NASA's Modern-Era Retrospective Analysis for Research and Applications (MERRA-Land [*Reichle et al.*, 2011]) precipitation and soil moisture data.

information comparable with other standardized indices such as SPI and SSI. Results indicate that MSDI provides objective drought information consistent with the USDM observations over the United States [*Hao and AghaKouchak*, 2014].

5. Research Gaps, Challenges, and Opportunities

5.1. Drought Impacts on the Carbon and Nitrogen Cycles

Many studies have evaluated the impact of drought on carbon cycles and ecosystems [*Poulter et al.*, 2014; *Yuan et al.*, 2014; *Yang et al.*, 2014; *Vicente-Serrano et al.*, 2012; *Asner et al.*, 2003, 2004]. Despite progress in monitoring and modeling terrestrial carbon and nitrogen cycles and budgets, the sensitivities of these cycles to climatic variability and extreme conditions still remain largely uncertain [*Gatti et al.*, 2014; *Phillips et al.*, 1998; *Huntingford et al.*, 2013]. Vegetation responds structurally and physiologically (e.g., by reducing their leaf cover) to droughts to minimize the effects of water stress, and longer and more severe droughts can lead to lasting changes in canopy structure, often facilitated by disturbance events including wildfire and outbreaks of insect pests [*Van der Molen et al.*, 2011; *Liu*, 2004; *Donohue et al.*, 2013; *Adams et al.*, 2009; *Donohue et al.*, 2009; *Dale et al.*, 2001; *Specht*, 1972; *O'grady et al.*, 2000; *Pook*, 1985, 1986; *Pook et al.*, 1997]. Droughts move the ecosystem overall to reduce CO_2 uptake, increasing CO_2 concentrations in the atmosphere [*Van der Molen et al.*, 2011; *Ciais et al.*, 2005; *Vetter et al.*, 2008; *Smith et al.*, 2010; *Van der Molen et al.*, 2011; *Meir et al.*, 2008; *Ciais et al.*, 2005]. The structural and physiological responses of plants and ecosystems to droughts could continue even after drought recovery [*Allen et al.*, 2010] and are not well understood at large scales. In energy-limited ecosystems, drought associated with less precipitation is normally accompanied with less cloud cover and hence more available energy for vegetation photosynthesis [*Huete et al.*, 2006; *Saleska et al.*, 2007]. Research in this direction can be supported and further enriched by satellite remote sensing observations.

Currently, carbon cycle and ecosystem models ingest satellite observations in combination with climate data from different sources to calculate measures of carbon fluxes including gross primary production (GPP), net primary production (NPP), and net ecosystem production (NEP). These measures of carbon cycling are used to quantify changes in response to variability in precipitation and temperature [*Running et al.*, 2004; *Justice et al.*, 2002; *Woodwell and Whittaker*, 1968; *Chapin III et al.*, 2006]. Several recent satellite missions and instruments provide measurements that can be used to calculate atmospheric CO_2 concentrations, including the Atmospheric Infrared Sounder (AIRS), Greenhouse Gases Observing Satellite (GOSAT), Tropospheric Emission Spectrometer (TES), GLOBALVIEW-CO2, Scanning Imaging Absorption Spectrometer for Atmospheric Cartography (SCIAMACHY), and the Orbiting Carbon Observatory 2 (OCO-2) - [*Miao et al.*, 2013]. These observations provide an opportunity to develop additional indicators to assist in monitoring drought effects on the carbon cycle and the terrestrial CO_2 budget. In addition, inverse modeling systems such as CarbonTracker assimilate satellite CO_2 observations and provide drought-relevant information. These new satellite instruments and data sets provide a unique opportunity to develop indicators to assist in monitoring drought effects on the carbon cycle and the terrestrial CO_2 budget and describe the functional relationships between water stress and changes in atmospheric CO_2 concentrations, particularly under climatic or hydrologic extremes such as drought.

While numerous drought indicators have been developed, limited studies have focused on indicators that are directly linked with GPP, NPP, NEP, or carbon and nitrogen cycling in terrestrial ecosystems. Changes in the carbon and nitrogen cycles are difficult to observe, monitor, and quantify. Most existing remote sensing-based drought indicators are not well suited or designed to monitor ecological responses to changes in carbon and nitrogen cycles, which can nevertheless have tremendous impacts on natural vegetation and ecosystem functions and services. Research on indicators that are linked with the carbon and nitrogen cycling can lead to a better understanding of the ecosystem response to droughts.

Drought effects on ecosystems are typically assessed relative to a long-term environmental baseline that can be affected by climatic change and variability, greenhouse gas emissions, and changes in the nitrogen and phosphorus cycles [*Donohue et al.*, 2013; *Wang et al.*, 2010; *Goll et al.*, 2014]. However, these relationships are not stationary. For example, with increasing atmospheric CO_2 concentrations, stomatal response, and vegetation water use efficiency are expected to change, an important ecosystem response that is detectable in water-limited ecosystems using long-term satellite and climate data records [*Donohue et al.*, 2013]. Ecosystem response to external forcings and climatic change in the baseline period can affect drought assessment. This highlights the importance of considering ecosystem changes in the baseline period when evaluating drought conditions. Having a wide variety of satellite observations offers the opportunity to develop methods that can accommodate and account for gradual changes over the period used to define a baseline for future monitoring and anomaly detection.

5.2. Combined Soil Moisture and Vegetation Water Content

Land surface parameters such as soil moisture and temperature are also important for drought assessment. Microwave brightness temperature is sensitive to land surface parameters (e.g., temperature and land cover) and provides valuable drought-relevant information (e.g., land cover, vegetation structure, temperature, soil moisture, and snow cover) [*Tedesco and Kim*, 2006]. Currently, the diurnal cycle of the microwave brightness temperature is available globally from a constellation of satellites [*Norouzi et al.*, 2012]. Studies show that densely vegetated regions with more moisture (including soil and vegetation moisture) exhibit a smaller diurnal microwave brightness temperature variation than other regions [*Norouzi et al.*, 2012; *Aires et al.*, 2004]. This implies that the diurnal variability of the microwave brightness temperature can potentially be used as an indicator of available combined soil moisture and vegetation water content and hence as a proxy for agricultural or ecosystem drought assessment.

It is worth pointing out that microwave brightness temperature is primarily controlled by land surface microwave emissivity and physical temperature [*Choudhury*, 1993; *Norouzi et al.*, 2011]. Changes in land surface parameters, including the moisture profile, affect the land surface microwave emissivity as well as the microwave brightness diurnal cycle [*Norouzi et al.*, 2014]. A major gap in current data sets is a lack of information on vertical moisture profiles in vegetation and soil. A recent study shows that the microwave land emissivity, derived from microwave temperature at a horizontal polarization, is substantially higher over densely vegetated areas [*Norouzi et al.*, 2012]. Also, the seasonal changes in vegetation density were found to be related to microwave land emissivity [*Norouzi et al.*, 2012]. The Soil Moisture Active Passive (SMAP) mission launched in January 2015, offers a unique avenue for future research in this direction. We believe that more research in this area could lead to a remotely sensed data set of vegetation density and moisture profiles (combined vegetation and soil) that can provide valuable information on water stress and droughts.

5.3. Microwave-Based Vegetation Indices

Vegetation indicators, such as NDVI obtained from optical satellite sensors, have been widely used to evaluate the impacts of droughts on ecosystems [*Tucker*, 1979]. Optical-based vegetation indicators provide valuable information on vegetation response to climate variability. However, they are sensitive to cloud cover, atmospheric effects, aerosols, water vapor, and land cover condition [*Andela et al.*, 2013; *Shi et al.*, 2008; *Liu et al.*, 2011b]. One limitation of the optical-based indicators is that they primarily provide information on conditions at the top of the canopy, especially in densely vegetated regions [*Shi et al.*, 2008]. A rapidly growing and influential area in remote sensing of drought is microwave-based vegetation monitoring [*Choudhury et al.*, 1987; *Andela et al.*, 2013; *Liu et al.*, 2013a; *Jones et al.*, 2011] that provides information on live aboveground biomass and canopy density. Unlike optical sensors, microwave sensors are less affected by atmospheric conditions and can penetrate into dense canopy. Furthermore, microwave sensors can collect information on vegetation conditions during both day and night [*Shi et al.*, 2008].

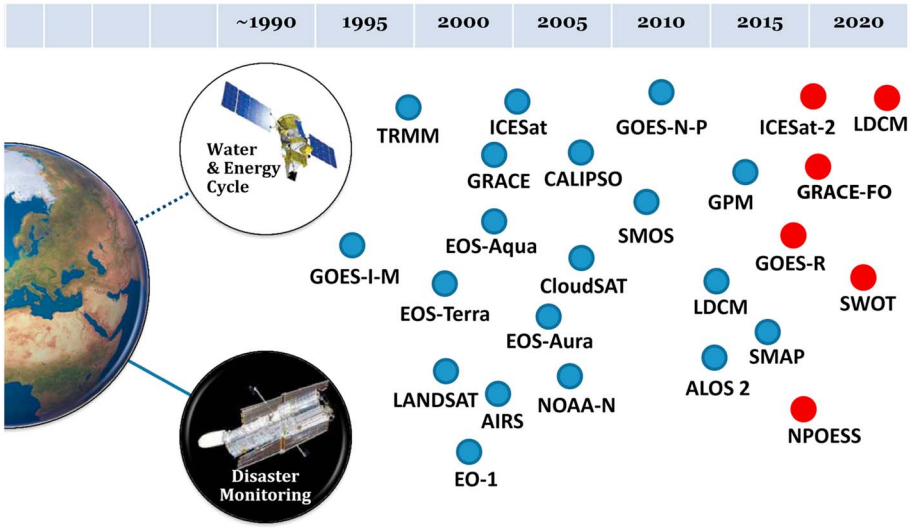

Figure 8. Current and future satellite missions relevant to drought monitoring and assessment (TRMM: Tropical Rainfall Measuring Mission; GRACE: Gravity Recovery and Climate Experiment; FO: FOllow-On; ICEsat: Ice, Clouds, and Land Elevation Satellite; CALIPSO: Cloud-Aerosol Lidar and Infrared Pathfinder Satellite Observations; EOS-Aqua: Earth Observing System Aqua; EOS-Terra: Earth Observing System Terra; EOS-Aura: Earth Observing System Aura; AIRS: Atmospheric Infrared Sounder; EO-1: Earth Observing-1; GOES: Geostationary Operational Environmental Satellite; NOAA-N: NOAA Polar Operational Environmental Satellites N Series; SMOS: Soil Moisture and Ocean Salinity satellite; ICESat-2: Ice, Clouds, and Land Elevation Satellite; GPM: Global Precipitation Measurement; LDCM: Landsat Data Continuity Mission; SWOT: Surface Water and Ocean Topography; SMAP: Soil Moisture Active Passive; ALOS 2: Advanced Land Observing Satellite; and NPOESS: National Polar-orbiting Operational Environmental Satellite System)—the list in not comprehensive.

We argue that high spatial resolution, microwave-based vegetation monitoring is one key to improving our understanding of drought impacts on ecosystem conditions, especially for monitoring vegetation response and carbon cycling specifically during drought events. The vegetation optical depth (VOD) [*Meesters et al.*, 2005; *Owe et al.*, 2001; *Jones et al.*, 2011; *Liu et al.*, 2011], for example, offers a unique approach for monitoring global phenology since it is sensitive to vegetation water content and canopy biomass. VOD has been extensively used to assess vegetation dynamics in drylands [*Andela et al.*, 2013], overgrazing [*Liu et al.*, 2013b], and start-of-season analysis [*Jones et al.*, 2011]. VOD and optical-based methods such as NDVI provide complementary information on the aboveground biomass and canopy top greenness, respectively [*Andela et al.*, 2013]. Combining the two approaches, interpreted in an ecohydrologically based data-driven framework, provides insights on the ecosystem response that cannot be achieved from each individual data set [*Andela et al.*, 2013]. Collectively, microwave sensors offer a relatively long-term record for investigating the impact and relative importance of droughts on global vegetation and biomass change. Future research in this direction can significantly improve our understanding of ecosystem responses to drought. The upcoming Global Ecosystem Dynamics Investigation lidar [*Dubayah et al.*, 2014], which is a laser-based instrument designed for 3-D analysis of Earth's forests, will also offer a unique avenue to monitor forest biomass and improve estimation of carbon fluxes.

5.4. Data Continuity, Consistency, and Management

Since the early 2000s, the number of satellite sensors and types of remote sensing observations have increased substantially, and many more are in the design and planning stages (see Figure 8 for a noncomprehensive list of missions). Some of the most important recent or upcoming missions relevant to drought monitoring include the Global Precipitation Mission (GPM), Geostationary Operational Environmental Satellites R series (GOES-R), GRACE Follow-On, SMAP, and SWOT missions (Figure 8). While these satellite missions provide opportunities to study droughts from different viewpoints, there are major challenges ahead such as data continuity, unquantified uncertainty, sensor changes, community acceptability, and data maintenance.

Data continuity is fundamental to the development of reliable satellite data records for drought applications. Most satellites are designed for less than a decade of operation, though many operate beyond their design life. Ideally, data sets should be extended through planning for follow-up missions. However, the planning,

approval, and design process for satellite missions can take decades and require substantial investments. The GPM, GOES-R, and GRACE Follow-On are examples of missions planned to avoid gaps in the current satellite-based precipitation and total water storage records. Another example is the Visible Infrared Imager Radiometer Suite (VIIRS) [*Justice et al.*, 2013; *Welsch et al.*, 2001; *Vargas et al.*, 2013], which is designed as the operational successor to MODIS and AVHRR. Long-term continuation of these and other satellite missions will remain an issue in the future as these systems age. The capability of extending multidecadal observations to develop robust drought climatologies remains uncertain.

Another major challenge is to ensure that the data volumes are well managed and that the data records are easily available to the science community and the public. This requires major hardware infrastructure to store and serve the data, and data professionals to process, curate, and disseminate the data. Securing funding for the required hardware and attracting long-term support for maintaining staff for data management are very challenging.

5.5. Multi-Index Composite Drought Monitoring

Recent studies show that combining multiple data sets improves drought detection [*Hao et al.*, 2014] and monitoring [*Mu et al.*, 2013]. Several multi-index (multisensor) drought monitoring indicators/frameworks have been developed to improve description of drought onset, development, and termination [*Keyantash and Dracup*, 2004; *Kao and Govindaraju*, 2010; *Tadesse et al.*, 2005; *Hao and AghaKouchak*, 2013; *Svoboda et al.*, 2002; *Rajsekhar et al.*, 2014]. Availability of multiple satellite data sets offers a unique avenue to explore multi-index or multivariate drought indicators.

Integration of snow into drought monitoring models is one of the least investigated areas and merits further exploration. The Snow and Cold Land Processes (SCLP) mission will provide microwave-based snow and snow water equivalent information [*Rott et al.*, 2010]. Integration of snow information into seasonal precipitation or runoff forecasts could lead to improvement in drought monitoring and seasonal prediction in regions that rely on snowmelt such as the western U.S. Multiple data sets describing different but interlinked environmental parameters provide the opportunity to develop advanced composite and multivariate (or multi-indicator) drought models, similar to the ones discussed in section 4.

Ground-based observations of many drought-related variables (e.g., snow, soil moisture, water vapor, and total water storage) are very limited or unevenly distributed across the world. This may limit development of multi-index indicators in data sparse regions. Given the variety of satellite observations (Figure 8), remote sensing allows development of an integrated multi-index composite drought assessment framework conceptually illustrated in Figure 9. However, multi-index and composite drought models are in their infancy, and more research is needed to develop robust statistical and mathematical frameworks for generating multi-index drought information.

5.6. Improving Early Drought Detection Using Satellite Observations

Early drought detection is fundamental to proactive decision making and disaster preparedness. Previous studies indicate that precipitation-based indicators (e.g., SPI) are better for drought detection compared to other indicators (e.g., SSI) [*Mo*, 2011; *Hao and AghaKouchak*, 2013]. A number of satellite missions and sensors (e.g., AIRS) provide near-surface air relative humidity information that is not currently being used for drought monitoring. Since near-surface air relative humidity directly influences evaporation and as such is connected to precipitation (integrated over period of time), it is reasonable to expect that it could provide valuable drought information and improve early drought onset detection.

Figure 10 displays the SPI and Standardized Relative Humidity Index (SRHI) [*Farahmand et al.*, 2014] derived by standardizing AIRS near-surface air relative humidity data using an empirical approach. Here a generalized empirical standardization approach is used that can be applied to different variables for deriving consistent drought indicators [*Farahmand and AghaKouchak*, 2014]. Figure 10 (left and right columns) show drought conditions based on SPI and SRHI in May and July 2010, respectively. The 2010 Russian drought signal can be observed in relative humidity data as well. Furthermore, in May 2010 and 2 months prior to the peak of the event, SRHI shows a stronger and more severe drought signal. All these indicators suggest that satellite-based relative humidity can provide an opportunity for early drought detection. This, however, requires more in-depth research on the consistency and reliability of relative humidity data for drought monitoring. In addition to relative humidity, there are many other satellite data sets that have not been fully explored for drought assessment, including water vapor, vapor pressure deficit, cloud cover, microwave

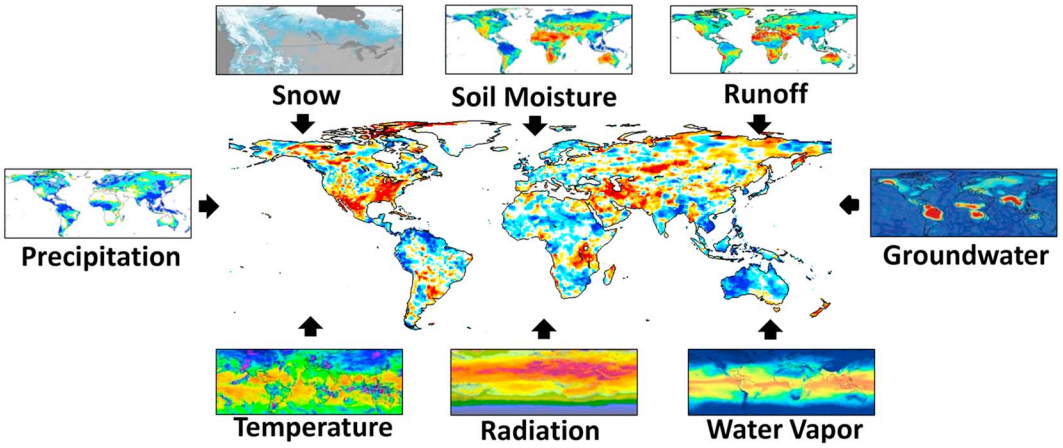

Figure 9. Multisensor (multi-index) composite drought monitoring using remote sensing observations: A schematic overview.

emissivity, microwave-based vegetation optical depth, and solar radiation. More research on such data sets could improve early drought detection or contribute to better monitoring of drought development.

5.7. Developing Climate Data Records

One of the major limitations of many of the currently available satellite data sets is their short length of record relative to meteorological stations, with Landsat, GOES, and AVHRR-MODIS-VIIRS as notable exceptions. Some of the relevant satellite missions and sensors (e.g., GRACE) provide only slightly over a decade of data, which may not be sufficient to study droughts from a climatological perspective, though they provide valuable information on anomalies for drought impact assessment [e.g., *Famiglietti and Rodell*, 2013]. Also, a number of satellite sensors are research instruments and there is no guarantee that the same (or sufficiently similar) instruments will be launched again to replace aging or failed instruments. Data continuity in the future largely relies on support for long-term investments in Earth observation satellites.

Lack of guaranteed support and commitment to invest in this field is a major roadblock for establishing consistent, long-term remote sensing data records necessary for accurate anomaly detection against a historical baseline. However, sensors that provide short-term records still provide valuable drought monitoring information, especially for drought impact assessment [*Rodell*, 2012; *Famiglietti and Rodell*, 2013]. There has been some work to create longer intersensor data records for key remote sensing variables, such as NDVI, by merging data from multiple satellite sensors such as AVHRR and MODIS [*Tucker et al.*, 2005; *Pinzon and Tucker*,

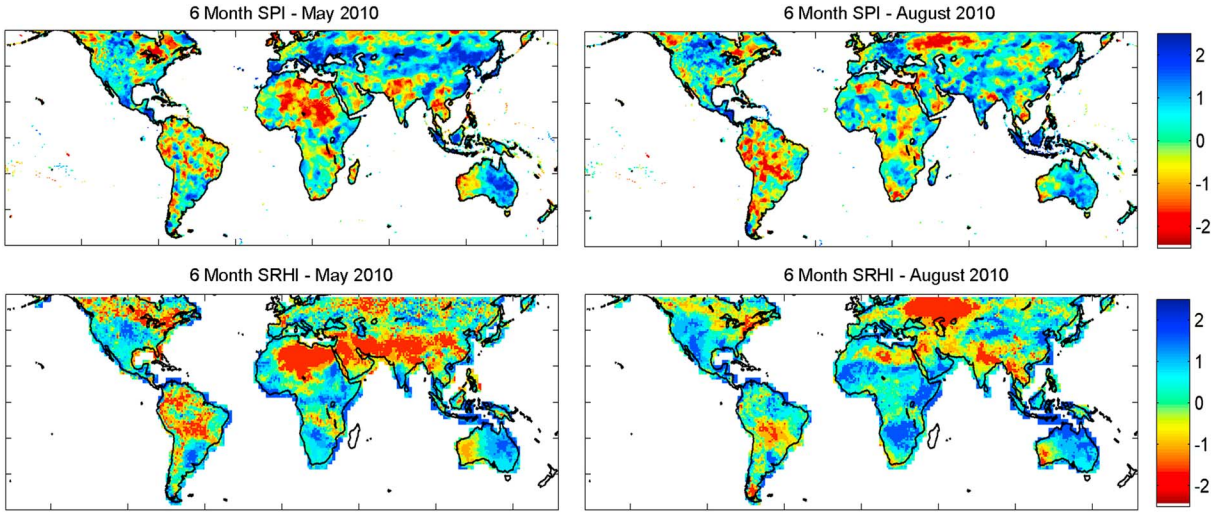

Figure 10. (top row) Standardized Precipitation Index (SPI) and (bottom row) Standardized Relative Humidity Index (SRHI) for (left column) May 2010 and (right column) August 2010.

2014; *Beck et al.*, 2011]. Effective models and algorithms need to combine multiple data sets [*AghaKouchak and Nakhjiri*, 2012] from different sources and/or assimilate satellite observations into model simulations [*Houborg et al.*, 2012; *Andreadis and Lettenmaier*, 2005; *Zaitchik et al.*, 2008] to generate long-term environmental and climate data records.

5.8. Uncertainty

Satellite data sets are subject to retrieval and sensor uncertainties that are often unquantified [*Dorigo et al.*, 2010; *Mehran and AghaKouchak*, 2014; *Pinker et al.*, 2009]. For this reason, several models and indicators have been developed for uncertainty assessment of satellite observations [*Gebremichael*, 2010; *Entekhabi et al.*, 2010b; *AghaKouchak and Mehran*, 2013; *Hossain and Huffman*, 2008]. However, most satellite-based data products still do not provide uncertainty estimates or bounds. Land surface and hydrologic models that use remote sensing data (as input or for data assimilation) are subject to other sources of error, including model structural and parameter uncertainties [*Li et al.*, 2012; *Dong et al.*, 2007; *Houborg et al.*, 2012]. Understanding input data uncertainty is fundamental to evaluating uncertainty of model-based simulations that use remote sensing information as input. Lack of uncertainty information may prevent integration of satellite data into decision making and operational applications.

More emphasis should be given to adequate characterization of the strengths and limitations of specific remote sensing tools and products, the results of which should be communicated to the general decision-making population in a nontechnical manner. Further research in uncertainty assessment is required to develop uncertainty products (bounds) for current and future satellite data sets. This will significantly improve the usability and acceptability of satellite observations within the hydrology community because these established bounds can provide guidance on the most appropriate times and locations to use data for a targeted decision-making process.

5.9. Community Acceptability

Product development as well as translating remote sensing observations and scientific data outputs in forms tailored for drought applications are critical for effective and sustained use within monitoring systems. This component of applied remote sensing is often overlooked but is essential in communicating valuable new information from new and emerging satellite-based systems and tools. Clearly defining basic elements, such as cartographic color schemes, summarization of retrieved information (e.g., estimated soil moisture versus soil moisture anomaly), and data formats, is one of the most important parts of the data-to-information process associated with development of remote sensing tools for the drought community. Engaging drought experts and key decision makers in this process is key to developing useful and applicable information from remote sensing that will be more widely accepted and integrated into operational drought monitoring and early warning systems.

6. Conclusion

Satellite remote sensing observations offer a unique toolset for studying droughts and their impacts on ecosystems. The unprecedented scale of available global observations have shed light on the biophysics of the drought phenomenon and have led to new drought indicators for research and practical applications. This study reviews the state-of-the-art remote sensing of drought from climatological and ecosystem perspectives and identifies a number of research gaps and opportunities, which are summarized below:

1. There are opportunities to develop new indicators that quantify the effects of drought on carbon and nitrogen cycling. Several recently launched satellite missions have provided atmospheric CO_2 information and offer an opportunity to develop indicators for assessing the relationships between water deficits and nutrient cycling. Such indicators would be fundamental to assessing drought and climate variability impacts on ecosystem and biogeochemical processes.
2. There is also a lack of indicators for assessing combined soil moisture and vegetation water content, and vertical profiles of moisture in vegetation. Recent advances in remote sensing of microwave land emissivity indicate that there are opportunities to quantitatively assess surface soil moisture and vegetation water content. We argue that microwave emissivity information could be used to develop an indicator of combined vegetation and soil water content.
3. Microwave-based vegetation monitoring offers a unique avenue for assessing drought impacts on vegetation dynamics and canopy density. Microwave and optical vegetation monitoring methods provide complementary information, and combining the two approaches leads to a better understanding of the

ecosystem response to climatic variability. Future research in this area can lead to a better understanding of drought impacts on ecosystems including changes in phenology, biomass, and carbon cycling.

4. Limited methods exist for deriving long-term climate data records using multiple satellite sensors. There are many satellite data sets that offer only a decade of observations (e.g., GRACE and AIRS) and thus cannot be used to assess an event from a historical climate perspective. This limitation can weaken the interpretation of indicators derived from the satellite data record. However, some of these data sets can be merged with other remote sensing data sets or reanalysis output to obtain long-term climate data records. Progress in this direction relies on development of robust statistical techniques for merging data records from different sensors.
5. There is a need to improve early drought detection by integrating satellite observations not currently used for drought monitoring (e.g., satellite near-surface air relative humidity and water vapor data). More research in this area could lead to major advancements in the field, particularly in drought early warning.
6. Developing statistical and mathematical frameworks for generating multi-index or composite drought information based on different satellite observations (e.g., precipitation, soil moisture, and relative humidity) presents a further opportunity. Limited statistical models are currently available for linking or merging different drought-related variables into one composite map.
7. Finally, uncertainty in this field is frequently unquantified. There are numerous satellite-based drought indicators that do not offer a quantitative measure of uncertainty. This is a roadblock for integrating remote sensing data into operational applications and decision-making processes. More research on uncertainty quantification will substantially improve the usability of satellite-based drought information.

Thus far, numerous remotely sensed drought indicators and models have been introduced that are not being used in current operational and decision-making systems. One of the key factors in using and accepting remotely sensed drought information is engaging decision makers in the process of model and indicator development. Community outreach and translation of remote sensing data into useful information for decision makers should be an integral part of the process. This is an important key to providing useful and valuable remote sensing information to the public.

Glossary

λ_{AET}	AET rate.
λ_{PET}	PET rate.
R_{VIS}	visible reflectance.
R_{mIR}	middle IR reflectance.
AIRS	Atmospheric Infrared Sounder.
ALEXI	Atmosphere-Land Exchange Inverse.
AET	actual ET.
AMSR	Advanced Microwave Scanning Radiometer–EOS.
AVHRR	advanced very high resolution radiometer.
CCI	Climate Change Initiative.
CLSM	Catchment land surface model.
CMORPH	CPC Morphing Technique.
CWSI	Crop Water Stress Index.
CTVI	Corrected Transformed Vegetation Index.
DDI	Distance Drought Index.
DSI	Drought Severity Index.
EDI	Evaporative Drought Index.
ESI	Evaporative Stress Index.
ET	evapotranspiration(mm/d).
ETM	Enhanced Thematic Mapper.
EVI	Enhanced Vegetation Index.
GEO	geostationary.
GIDMaPS	Global Integrated Drought Monitoring and Prediction System.
GOES-R	Geostationary Operational Environmental Satellites R series.
GOSAT	Greenhouse Gases Observing Satellite.
GPCP	Global Precipitation Climatology Project.

GPM	Global Precipitation Mission.
GPP	gross primary production.
GRACE	Gravity Recovery and Climate Experiment.
GRACE-DAS	GRACE data assimilation system.
IPAD	International Production Assessment Division.
IR	infrared.
LEO	low Earth orbit.
LST	land surface temperature.
MIDI	Microwave Integrated Drought Index.
MSDI	Multivariate Standardized Drought Index.
MODIS	Moderate Resolution Imaging Spectroradiometer.
MPDI	Modified Perpendicular Drought Index.
MW	microwave.
NDDI	Normalized Difference Drought Index.
NDVI	normalized difference vegetation index.
NDWI	Normalized Difference Water Index.
NEP	net ecosystem production.
NIR	near infrared.
NMDI	Normalized Multi-band Drought Index.
NPP	net primary production.
NRVI	Normalized Ratio Vegetation Index.
NSDI	Normalized Difference Snow Index.
P	precipitation.
PCI	Precipitation Condition Index.
PDI	Perpendicular Drought Index.
PERSIANN	Precipitation Estimation from Remotely Sensed Information using Artificial Neural Networks
PET	potential ET.
PVI	Perpendicular Vegetation Index.
SM	soil moisture.
PDSI	Palmer Drought Severity Index.
PNP	Percent of Normal Precipitation.
R	red.
RDI	Reconnaissance Drought Index.
SA	snow albedo.
SAVI	Soil-Adjusted Vegetation Index.
SCA	snow-covered area.
SCIAMACHY	Scanning Imaging Absorption Spectrometer for Atmospheric Cartography.
SCLP	Snow and Cold Land Processes.
SD	snow depth.
SMCI	Soil Moisture Condition Index.
SDCI	Scaled Drought Condition Index.
SPI	Standardized Precipitation Index.
SSI	Standardized Soil Moisture Index.
SRHI	Standardized Relative Humidity Index.
SVI	Standardized Vegetation Index.
SWE	snow water equivalent.
SWIR	shortwave infrared.
TCA	triple collocation analysis.
TCI	Temperature Condition Index.
TES	Tropospheric Emission Spectrometer.
TIR	thermal infrared.
TIROS-1	Television and Infrared Observation Satellite.
TM	Landsat thematic mapper.
TMPA	Multi-satellite Precipitation Analysis.
TRMM	Tropical Rainfall Measuring Mission.

TTVI	Thiam's Transformed Vegetation Index.
TVI	Transformed Vegetation Index.
TWS	terrestrial water storage.
USDA	United States Department of Agriculture.
USDM	United States Drought Monitor.
VCI	Vegetation Condition Index.
VegDRI	Vegetation Drought Response Index.
VIIRS	Visible Infrared Imager Radiometer Suite.
VIS	visible.
VTCI	Vegetation Temperature Condition Index.
WACMOS	Water Cycle Multi-Mission Observation Strategy.
WDI	Water Deficit Index.
WMO	World Meteorological Organization.

Acknowledgments
This study is supported by the National Aeronautics and Space Administration (NASA) award NNX15AC27G. The input data sets and final outputs presented in this paper are all freely available through the Global Integrated Drought Monitoring and Prediction System (GIDMaPS; http://drought.eng.uci.edu/), and the NOAA/NIDIS Global Vegetation Health data (http://www.star.nesdis.noaa.gov/smcd/emb/vci/VH/).

The Editor of this manuscript was Gregory Okin. He thanks three anonymous reviewers for their assistance in reviewing the manuscript.

References

Adams, H. D., M. Guardiola-Claramonte, G. A. Barron-Gafford, J. C. Villegas, D. D. Breshears, C. B. Zou, P. A. Troch, and T. E. Huxman (2009), Temperature sensitivity of drought-induced tree mortality portends increased regional die-off under global-change-type drought, *Proc. Nat. Acad. Sci.*, *106*(17), 7063–7066, doi:10.1073/pnas.0901438106.

Adegoke, J. O., and A. M. Carleton (2002), Relations between soil moisture and satellite vegetation indices in the US corn belt, *J. Hydrometeorol.*, *3*(4), 395–405, doi:10.1175/1525-7541(2002)003<0395:RBSMAS>2.0.CO;2.

Adler, R., et al. (2003), The version-2 Global Precipitation Climatology Project (GPCP) monthly precipitation analysis (1979–present), *J. Hydrometeorol.*, *4*(6), 1147–1167, doi:10.1175/1525-7541(2003)004<1147:TVGPCP>2.0.CO;2.

AghaKouchak, A. (2014a), A baseline probabilistic drought forecasting framework using Standardized Soil Moisture Index: Application to the 2012 United States drought, *Hydrol. Earth Syst. Sci.*, *18*(7), 2485–2492, doi:10.5194/hess-18-2485-2014.

AghaKouchak, A. (2014b), A multivariate approach for persistence-based drought prediction: Application to the 2010–2011 East Africa drought, *J. Hydrol.*, *526*, 127–135, doi:10.1016/j.jhydrol.2014.09.063.

AghaKouchak, A., and A. Mehran (2013), Extended contingency table: Performance metrics for satellite observations and climate model simulations, *Water Resour. Res.*, *49*(10), 7144–7149, doi:10.1002/wrcr.20498.

AghaKouchak, A., and N. Nakhjiri (2012), A near real-time satellite-based global drought climate data record, *Environ. Res. Lett.*, *7*(4), 044037, doi:10.1088/1748-9326/7/4/044037.

AghaKouchak, A., A. Mehran, H. Norouzi, and A. Behrangi (2012), Systematic and random error components in satellite precipitation data sets, *Geophys. Res. Lett.*, *39*, L09406, doi:10.1029/2012GL051592.

Aghakouchak, A., L. Cheng, O. Mazdiyasni, and A. Farahmand (2014), Global warming and changes in risk of concurrent climate extremes: Insights from the 2014 California drought, *Geophys. Res. Lett.*, *41*, 8847–8852, doi:10.1002/2014GL062308.

Aires, F., C. Prigent, and W. Rossow (2004), Temporal interpolation of global surface skin temperature diurnal cycle over land under clear and cloudy conditions, *J. Geophys. Res.*, *109*, D04313, doi:10.1029/2003JD003527.

Allen, C. D., et al. (2010), A global overview of drought and heat-induced tree mortality reveals emerging climate change risks for forests, *For. Ecol. Manage.*, *259*(4), 660–684, doi:10.1016/j.foreco.2009.09.001.

Allen, R., L. Pereira, D. Raes, and M. Smith (1998), Crop evapotranspiration—Guidelines for computing crop water requirements—FAO Irrigation and drainage paper 56, *Tech. Rep.*

Allen, R. G., M. Tasumi, and R. Trezza (2007), Satellite-based energy balance for mapping evapotranspiration with internalized calibration (METRIC) model, *J. Irrig. Drain. Eng.*, *133*(4), 380–394, doi:10.1061/(ASCE)0733-9437(2007)133:4(380).

Ambaw, G. M. (2013), Satellite based remote sensing of soil moisture for drought detection and monitoring in the horn of Africa, PhD thesis, Politecnico di Torino, Turin, Italy. [Available at http://porto.polito.it/2507436/.]

Andela, N., Y. Y. Liu, A. I. J. M. van Dijk, R. A. M. de Jeu, and T. R. McVicar (2013), Global changes in dryland vegetation dynamics (1988–2008) assessed by satellite remote sensing: Comparing a new passive microwave vegetation density record with reflective greenness data, *Biogeosci. Discuss.*, *10*(5), 8749–8797, doi:10.5194/bg-10-6657-2013.

Anderson, L., Y. Malhi, L. Aragao, and S. Saatchi (2008), Spatial patterns of the canopy stress during 2005 drought in Amazonia, *Geoscience and Remote Sensing Symposium, 2007. IGARSS 2007. IEEE International*, pp. 2294–2297, Barcelona, Spain, doi:10.1109/IGARSS.2007.4423299.

Anderson, M., J. Norman, G. Diak, W. Kustas, and J. Mecikalski (1997), A two-source time-integrated model for estimating surface fluxes using thermal infrared remote sensing, *Remote Sens. Environ.*, *60*(2), 195–216, doi:10.1016/S0034-4257(96)00215-5.

Anderson, M. C., and W. P. Kustas (2008), Thermal remote sensing of drought and evapotranspiration, *Eos Trans. AGU*, *89*(26), 233–234, doi:10.1029/2008EO260001.

Anderson, M. C., J. M. Norman, J. R. Mecikalski, J. A. Otkin, and W. P. Kustas (2007), A climatological study of evapotranspiration and moisture stress across the continental United States based on thermal remote sensing: 1. Model formulation, *J. Geophys. Res.*, *112*, D10117, doi:10.1029/2006JD007506.

Anderson, M. C., et al. (2011a), Mapping daily evapotranspiration at field to continental scales using geostationary and polar orbiting satellite imagery, *Hydrol. Earth Syst. Sci.*, *15*(1), 223–239, doi:10.5194/hess-15-223-2011.

Anderson, M. C., C. Hain, B. Wardlow, A. Pimstein, J. R. Mecikalski, and W. P. Kustas (2011b), Evaluation of drought indices based on thermal remote sensing of evapotranspiration over the continental United States, *J. Clim.*, *24*(8), 2025–2044, doi:10.1175/2010JCLI3812.1.

Anderson, M. C., C. Hain, B. Wardlow, A. Pimstein, J. Mecikalski, and W. Kustas (2012), A thermal-based evaporative stress index for monitoring surface moisture depletion, in *Remote Sensing of Drought: Innovative Monitoring Approaches*, pp. 145–167, CRC Press.

Anderson, M. C., C. Cammalleri, C. R. Hain, J. Otkin, X. Zhan, and W. Kustas (2013a), Using a diagnostic soil-plant-atmosphere model for monitoring drought at field to continental scales, *Procedia Environ. Sci.*, *19*, 47–56, doi:10.1016/j.proenv.2013.06.006.

Anderson, M. C., C. Hain, J. Otkin, X. Zhan, K. Mo, M. Svoboda, B. Wardlow, and A. Pimstein (2013b), An intercomparison of drought indicators based on thermal remote sensing and NLDAS-2 simulations with US Drought Monitor classifications, *J. Hydrometeorol.*, *14*(4), 1035–1056, doi:10.1175/JHM-D-12-0140.1.

Anderson, W. B., B. Zaitchik, C. Hain, M. Anderson, M. Yilmaz, J. Mecikalski, and L. Schultz (2012), Towards an integrated soil moisture drought monitor for East Africa, *Hydrol. Earth Syst. Sci.*, *16*(8), 2893–2913, doi:10.5194/hess-16-2893-2012.

Andreadis, K. M., and D. Lettenmaier (2005), Assimilating passive microwave brightness temperature for snow water equivalent estimation, *AMS Annual Meeting, 19th Conference on Hydrology*, San Diego, Calif.

Arkin, P. A., R. Joyce, and J. E. Janowiak (1994), The estimation of global monthly mean rainfall using infrared satellite data: The GOES Precipitation Index (GPI), *Remote Sens. Rev.*, *11*(1–4), 107–124, doi:10.1080/02757259409532261.

Asner, G. P., and A. Alencar (2010), Drought impacts on the Amazon forest: The remote sensing perspective, *New Phytol.*, *187*(3), 569–578, doi:10.1111/j.1469-8137.2010.03310.x.

Asner, G. P., S. Archer, R. F. Hughes, R. J. Ansley, and C. A. Wessman (2003), Net changes in regional woody vegetation cover and carbon storage in Texas drylands, 1937–1999, *Global Change Biol.*, *9*(3), 316–335, doi:10.1046/j.1365-2486.2003.00594.x.

Asner, G. P., D. Nepstad, G. Cardinot, and D. Ray (2004), Drought stress and carbon uptake in an Amazon forest measured with spaceborne imaging spectroscopy, *Proc. Natl. Acad. Sci. U.S.A.*, *101*(16), 6039–6044, doi:10.1073/pnas.0400168101.

Asrar, G., M. Fuchs, E. Kanemasu, and J. Hatfield (1984), Estimating absorbed photosynthetic radiation and leaf area index from spectral reflectance in wheat, *Agron. J.*, *76*(2), 300–306, doi:10.2134/agronj1984.00021962007600020029x.

Asrar, G., R. B. Myneni, and E. T. Kanemasu (1989), Estimation of plant-canopy attributes from spectral reflectance measurements, in *Theory and Applications of Optical Remote Sensing*, edited by G. Asrar, pp. 252–296, John Wiley, New York.

Bales, R. C., N. P. Molotch, T. H. Painter, M. D. Dettinger, R. Rice, and J. Dozier (2006), Mountain hydrology of the western United States, *Water Resour. Res.*, *42*, W08432, doi:10.1029/2005WR004387.

Baret, F., and G. Guyot (1991), Potentials and limits of vegetation indices for LAI and APAR assessment, *Remote Sens. Environ.*, *35*(2), 161–173, doi:10.1016/0034-4257(91)90009-U.

Barrett, E., and R. Herschy (1989), Opportunities for satellite remote sensing in hydrology and water management, *Geocarto Int.*, *4*(2), 11–18, doi:10.1080/10106048909354204.

Barrett, E., M. Beaumont, and R. Herschy (1990), Satellite remote sensing for operational hydrology: Present needs and future opportunities, *Remote Sens. Rev.*, *4*(2), 451–466, doi:10.1080/02757259009532113.

Bayarjargal, Y., A. Karnieli, M. Bayasgalan, S. Khudulmur, C. Gandush, and C. J. Tucker (2006), A comparative study of NOAA–AVHRR derived drought indices using change vector analysis, *Remote Sens. Environ.*, *105*(1), 9–22, doi:10.1016/j.rse.2006.06.003.

Beck, H. E., T. R. McVicar, A. I. Dijk, J. Schellekens, R. A. de Jeu, and L. A. Bruijnzeel (2011), Global evaluation of four AVHRR-NDVI data sets: Intercomparison and assessment against Landsat imagery, *Remote Sens. Environ.*, *115*(10), 2547–2563, doi:10.1016/j.rse.2011.05.012.

Boken, V. K., et al. (2005), *Monitoring and Predicting Agricultural Drought: A Global Study*, p. 496, Oxford Univ. Press, New York.

Bolten, J. D., W. T. Crow, X. Zhan, T. J. Jackson, and C. A. Reynolds (2010), Evaluating the utility of remotely sensed soil moisture retrievals for operational agricultural drought monitoring, *IEEE J. Sel. Top. Appl. Earth Obs. Remote Sens.*, *3*(1), 57–66, doi:10.1109/JSTARS.2009.2037163.

Bromwich, D. H., et al. (2012), Tropospheric clouds in Antarctica, *Rev. Geophys.*, *50*, RG1004, doi:10.1029/2011RG000363.

Brown, J. F., B. D. Wardlow, T. Tadesse, M. J. Hayes, and B. C. Reed (2008), The Vegetation Drought Response Index (VegDRI): A new integrated approach for monitoring drought stress in vegetation, *GISci. Remote Sens.*, *45*(1), 16–46, doi:10.2747/1548-1603.45.1.16.

Caccamo, G., L. Chisholm, R. A. Bradstock, and M. Puotinen (2011), Assessing the sensitivity of MODIS to monitor drought in high biomass ecosystems, *Remote Sens. Environ.*, *115*(10), 2626–2639, doi:10.1016/j.rse.2011.05.018.

Carlson, T. (2007), An overview of the "triangle method" for estimating surface evapotranspiration and soil moisture from satellite imagery, *Sensors*, *7*(8), 1612–1629.

Cashion, J., V. Lakshmi, D. Bosch, and T. J. Jackson (2005), Microwave remote sensing of soil moisture: Evaluation of the TRMM microwave imager (TMI) satellite for the Little River Watershed Tifton, Georgia, *J. Hydrol.*, *307*(1), 242–253, doi:10.1016/j.jhydrol.2004.10.019.

Chapin III, F., et al. (2006), Reconciling carbon-cycle concepts, terminology, and methods, *Ecosystems*, *9*(7), 1041–1050, doi:10.1007/s10021-005-0105-7.

Chappell, A., L. J. Renzullo, T. H. Raupach, and M. Haylock (2013), Evaluating geostatistical methods of blending satellite and gauge data to estimate near real-time daily rainfall for Australia, *J. Hydrol.*, *493*(17), 105–114, doi:10.1016/j.jhydrol.2013.04.024.

Chen, D., J. Huang, and T. J. Jackson (2005), Vegetation water content estimation for corn and soybeans using spectral indices derived from MODIS near-and short-wave infrared bands, *Remote Sens. Environ.*, *98*(2), 225–236, doi:10.1016/j.rse.2005.07.008.

Chen, J., C. Wilson, B. Tapley, Z. Yang, and G. Niu (2009), 2005 drought event in the Amazon River basin as measured by GRACE and estimated by climate models, *J. Geophys. Res.*, *114*, B05404, doi:10.1029/2008JB006056.

Choi, M., J. Jacobs, M. Anderson, and D. Bosch (2013), Evaluation of drought indices via remotely sensed data with hydrological variables, *J. Hydrol.*, *476*(7), 265–273, doi:10.1016/j.jhydrol.2012.10.042.

Choudhury, B., C. Tucker, R. Golus, and W. Newcomb (1987), Monitoring vegetation using Nimbus-7 scanning multichannel microwave radiometer's data, *Int. J. Remote Sens.*, *8*(3), 533–538, doi:10.1080/01431168708948660.

Choudhury, B. J. (1993), Reflectivities of selected land surface types at 19 and 37 GHz from SSM/I observations, *Remote Sens. Environ.*, *46*(1), 1–17, doi:10.1016/0034-4257(93)90028-V.

Ciais, P., et al. (2005), Europe-wide reduction in primary productivity caused by the heat and drought in 2003, *Nature*, *437*(7058), 529–533, doi:10.1038/nature03972.

Dale, V. H., et al. (2001), Climate change and forest disturbances: Climate change can affect forests by altering the frequency, intensity, duration, and timing of fire, drought, introduced species, insect and pathogen outbreaks, hurricanes, windstorms, ice storms, or landslides, *BioScience*, *51*(9), 723–734, doi:10.1641/0006-3568(2001)051[0723:CCAFD]2.0.CO;2.

Dalezios, N., A. Blanta, and N. Spyropoulos (2012), Assessment of remotely sensed drought features in vulnerable agriculture, *Nat. Hazard. Earth Syst. Sci.*, *12*(10), 3139–3150, doi:10.5194/nhess-12-3139-2012.

Damberg, L., and A. AghaKouchak (2014), Global trends and patterns of drought from space, *Theor. Appl. Climatol.*, *117*(3), 441–448, doi:10.1007/s00704-013-1019-5.

Deering, D., and J. Rouse (1975), Measuring "forage production" of grazing units from landsat MSS data, *10th International Symposium on Remote Sensing of Environment, Ann Arbor, Mich*, pp. 1169–1178.

Di, L., D. C. Rundquist, and L. Han (1994), Modelling relationships between NDVI and precipitation during vegetative growth cycles, *Int. J. Remote Sens.*, *15*(10), 2121–2136, doi:10.1080/01431169408954231.

D'Odorico, P., K. Caylor, G. S. Okin, and T. M. Scanlon (2007), On soil moisture-vegetation feedbacks and their possible effects on the dynamics of dryland ecosystems, *J. Geophys. Res.*, *112*, G04010, doi:10.1029/2006JG000379.

Dong, J., J. P. Walker, P. R. Houser, and C. Sun (2007), Scanning multichannel microwave radiometer snow water equivalent assimilation, *J. Geophys. Res.*, *112*, D07108, doi:10.1029/2006JD007209.

Donohue, R. J., T. McVicar, and M. L. Roderick (2009), Climate-related trends in Australian vegetation cover as inferred from satellite observations, 1981–2006, *Global Change Biol.*, *15*(4), 1025–1039, doi:10.1111/j.1365-2486.2008.01746.x.
Donohue, R. J., T. R. McVicar, and M. L. Roderick (2010), Assessing the ability of potential evaporation formulations to capture the dynamics in evaporative demand within a changing climate, *J. Hydrol.*, *386*(1), 186–197, doi:10.1016/j.jhydrol.2010.03.020.
Donohue, R. J., M. L. Roderick, T. R. McVicar, and G. D. Farquhar (2013), Impact of CO2 fertilization on maximum foliage cover across the globe's warm, arid environments, *Geophys. Res. Lett.*, *40*, 3031–3035, doi:10.1002/grl.50563.
Dorigo, W., K. Scipal, R. Parinussa, Y. Liu, W. Wagner, R. De Jeu, and V. Naeimi (2010), Error characterisation of global active and passive microwave soil moisture datasets, *Hydrol. Earth Syst. Sci.*, *14*(12), 2605–2616, doi:10.5194/hess-14-2605-2010.
Dozier, J., R. O. Green, A. W. Nolin, and T. H. Painter (2009), Interpretation of snow properties from imaging spectrometry, *Remote Sens. Environ.*, *113*(1), S25–S37, doi:10.1016/j.rse.2007.07.029.
Dubayah, R., et al. (2014), The Global Ecosystem Dynamics Investigation (GEDI) lidar, *ForestSAT2014 Open Conference System, 4-7 November 2014, Riva del Garda, Italy*.
Durand, M., N. P. Molotch, and S. A. Margulis (2008), Merging complementary remote sensing datasets in the context of snow water equivalent reconstruction, *Remote Sens. Environ.*, *112*(3), 1212–1225, doi:10.1016/j.rse.2007.08.010.
Durand, M., E. J. Kim, and S. A. Margulis (2008), Quantifying uncertainty in modeling snow microwave radiance for a mountain snowpack at the point-scale, including stratigraphic effects, *IEEE Trans. Geosci. Remote Sens.*, *46*(6), 1753–1767, doi:10.1109/TGRS.2008.916221.
Easterling, D. (2013), Global data sets for analysis of climate extremes, *Extremes Changing Clim.*, *65*, 347–361, doi:10.1007/978-94-007-4479-012.
Ebert, E., J. Janowiak, and C. Kidd (2007), Comparison of near real time precipitation estimates from satellite observations and numerical models, *Bull. Am. Meteorol. Soc.*, *88*(1), 47–64, doi:10.1175/BAMS-88-1-47.
Entekhabi, D., et al. (2004), The hydrosphere state (Hydros) satellite mission: An Earth system pathfinder for global mapping of soil moisture and land freeze/thaw, *IEEE Trans. Geosci. Remote Sens.*, *42*(10), 2184–2195, doi:10.1109/TGRS.2004.834631.
Entekhabi, D., et al. (2010a), The soil moisture active passive (SMAP) mission, *Proc. IEEE*, *98*(5), 704–716, doi:10.1109/JPROC.2010.2043918.
Entekhabi, D., R. H. Reichle, R. D. Koster, and W. T. Crow (2010b), Performance metrics for soil moisture retrievals and application requirements, *J. Hydrometeorol.*, *11*(3), 832–840, doi:10.1175/2010JHM1223.1.
Famiglietti, J. S., and M. Rodell (2013), Water in the balance, *Science*, *340*(6138), 1300–1301, doi:10.1126/science.1236460.
Farahmand, A., and A. AghaKouchak (2014), A generalized framework for deriving nonparametric standardized drought indicators, *Adv. Water Res.*, *76*, 140–145, doi:10.1016/j.advwatres.2014.11.012.
Farahmand, A., J. Teixeira, and A. AghaKouchak (2014), A vantage from space can detect earlier drought onset: An approach using relative humidity, *Sci. Rep.*, *5*, 8553, doi:10.1038/srep08553.
Farrar, T., S. Nicholson, and A. Lare (1994), The influence of soil type on the relationships between NDVI, rainfall, and soil moisture in semiarid Botswana. II. NDVI response to soil moisture, *Remote Sens. Environ.*, *50*(2), 121–133, doi:10.1016/0034-4257(94)90039-6.
Fensholt, R., I. Sandholt, S. Stisen, and C. Tucker (2006), Analysing NDVI for the African continent using the geostationary METEOSAT second generation SEVIRI sensor, *Remote Sens. Environ.*, *101*(2), 212–229, doi:10.1016/j.rse.2005.11.013.
Foster, J. L., C. Sun, J. P. Walker, R. Kelly, A. Chang, J. Dong, and H. Powell (2005), Quantifying the uncertainty in passive microwave snow water equivalent observations, *Remote Sens. Environ.*, *94*(2), 187–203, doi:10.1016/j.rse.2004.09.012.
Foster, J. L., et al. (2011), A blended global snow product using visible, passive microwave and scatterometer satellite data, *Int. J. Remote Sens.*, *32*(5), 1371–1395, doi:10.1080/01431160903548013.
Funk, C. (2011), We thought trouble was coming, *Nature*, *476*(7358), 7, doi:10.1038/476007a.
Funk, C., and M. E. Budde (2009), Phenologically-tuned MODIS NDVI-based production anomaly estimates for Zimbabwe, *Remote Sens. Environ.*, *113*(1), 115–125, doi:10.1016/j.rse.2008.08.015.
Gallagher, J., P. Biscoe, and B. Hunter (1976), Effects of drought on grain growth, *Nature*, *264*, 541–542.
Gao, B.-C. (1996), NDWI a normalized difference water index for remote sensing of vegetation liquid water from space, *Remote Sens. Environ.*, *58*(3), 257–266, doi:10.1038/264541a0.
Gatti, L., et al. (2014), Drought sensitivity of Amazonian carbon balance revealed by atmospheric measurements, *Nature*, *506*(7486), 76–80, doi:10.1038/nature12957.
Gebremichael, M. (2010), Framework for satellite rainfall product evaluation, *Geophys. Monogr. Ser.*, *191*, 265–275, doi:10.1029/2010GM000974.
Ghulam, A., Q. Qin, and Z. Zhan (2007a), Designing of the perpendicular drought index, *Environ. Geol.*, *52*(6), 1045–1052, doi:10.1007/s00254-006-0544-2.
Ghulam, A., Q. Qin, T. Teyip, and Z. -L. Li (2007b), Modified perpendicular drought index (MPDI): A real-time drought monitoring method, *ISPRS J. Photogramm. Remote Sens.*, *62*(2), 150–164, doi:10.1016/j.isprsjprs.2007.03.002.
Glenn, E. P., A. R. Huete, P. L. Nagler, K. K. Hirschboeck, and P. Brown (2007), Integrating remote sensing and ground methods to estimate evapotranspiration, *Crit. Rev. Plant Sci.*, *26*(3), 139–168, doi:10.1080/07352680701402503.
Glenn, E. P., C. M. Neale, D. J. Hunsaker, and P. L. Nagler (2011), Vegetation index-based crop coefficients to estimate evapotranspiration by remote sensing in agricultural and natural ecosystems, *Hydrol. Processes*, *25*(26), 4050–4062, doi:10.1002/hyp.8392.
Godfray, H. C. J., J. R. Beddington, I. R. Crute, L. Haddad, D. Lawrence, J. F. Muir, J. Pretty, S. Robinson, S. M. Thomas, and C. Toulmin (2010), Food security: The challenge of feeding 9 billion people, *Science*, *327*(5967), 812–818, doi:10.1126/science.1185383.
Golian, S., O. Mazdiyasni, and A. AghaKouchak (2014), Trends in meteorological and agricultural droughts in Iran, *Theor. Appl. Climatol.*, *119*(3–4), 679–688, doi:10.1007/s00704-014-1139-6.
Goll, D. S., N. Moosdorf, J. Hartmann, and V. Brovkin (2014), Climate-driven changes in chemical weathering and associated phosphorus release since 1850: Implications for the land carbon balance, *Geophys. Res. Lett.*, *41*, 3553–3558, doi:10.1002/2014GL059471.
Goodison, B. E. (1989), Determination of areal snow water equivalent on the Canadian prairies using passive microwave satellite data, in *Geoscience and Remote Sensing Symposium, 1989. IGARSS'89. 12th Canadian Symposium on Remote Sensing*, vol. 3, pp. 1243–1246, IEEE.
Grasso, V. F., and A. Singh (2011), Early warning systems: State-of-art analysis and future directions, United Nations Environment Programme (UNEP). [Available at http://na.unep.net/siouxfalls/publications/Early_Warning.pdf.]
Grody, N. C., and A. N. Basist (1996), Global identification of snowcover using SSM/I measurements, *IEEE Trans. Geosci. Remote Sens.*, *34*(1), 237–249, doi:10.1109/36.481908.
Gruhier, C., et al. (2010), Soil moisture active and passive microwave products: Intercomparison and evaluation over a Sahelian site, *Hydrol. Earth Syst. Sci.*, *14*, 141–156, doi:10.5194/hess-14-141-2010.
Gu, Y., J. F. Brown, J. P. Verdin, and B. Wardlow (2007), A five-year analysis of MODIS NDVI and NDWI for grassland drought assessment over the central Great Plains of the United States, *Geophys. Res. Lett.*, *34*, L06407, doi:10.1029/2006GL029127.

Gu, Y., E. Hunt, B. Wardlow, J. B. Basara, J. F. Brown, and J. P. Verdin (2008), Evaluation of MODIS NDVI and NDWI for vegetation drought monitoring using Oklahoma Mesonet soil moisture data, *Geophys. Res. Lett.*, *35*, L22401, doi:10.1029/2008GL035772.
Guan, B., N. P. Molotch, D. E. Waliser, S. M. Jepsen, T. H. Painter, and J. Dozier (2013), Snow water equivalent in the Sierra Nevada: Blending snow sensor observations with snowmelt model simulations, *Water Resour. Res.*, *49*, 5029–5046, doi:10.1002/wrcr.20387.
Gutman, G. G. (1990), Towards monitoring droughts from space, *J. Clim.*, *3*(2), 282–295, doi:10.1175/1520-0442(1990)003<0282:TMDFS>2.0.CO;2.
Hall, D. K., G. A. Riggs, V. V. Salomonson, N. E. DiGirolamo, and K. J. Bayr (2002), MODIS snow-cover products, *Remote Sens. Environ.*, *83*(1), 181–194, doi:10.1016/S0034-4257(02)00095-0.
Hao, Z., and A. AghaKouchak (2013), Multivariate standardized drought index: A parametric multi-index model, *Adv. Water Res.*, *57*, 12–18, doi:10.1016/j.advwatres.2013.03.009.
Hao, Z., and A. AghaKouchak (2014), A nonparametric multivariate multi-index drought monitoring framework, *J. Hydrometeorol.*, *15*, 89–101, doi:10.1175/JHM-D-12-0160.1.
Hao, Z., and V. P. Singh (2015), Drought characterization from a multivariate perspective: A review, *J. Hydrol.*, *527*, 668–678.
Hao, Z., A. AghaKouchak, N. Nakhjiri, and A. Farahmand (2014), Global Integrated Drought Monitoring and Prediction System, *Sci. Data*, *1*, 140001, doi:10.1038/sdata.2014.1.
He, M., T. S. Hogue, S. A. Margulis, and K. J. Franz (2012), An integrated uncertainty and ensemble-based data assimilation approach for improved operational streamflow predictions, *Hydrol. Earth Syst. Sci.*, *16*(3), 815–831, doi:10.5194/hess-16-815-2012.
Hatfield, J., G. Asrar, and E. Kanemasu (1984), Intercepted photosynthetically active radiation estimated by spectral reflectance, *Remote Sens. Environ.*, *14*(1), 65–75, doi:10.1016/0034-4257(84)90008-7.
Hayes, M., M. Svoboda, D. Wilhite, and O. Vanyarkho (1999), Monitoring the 1996 drought using the Standardized Precipitation Index, *Bull. Am. Meteorol. Soc.*, *80*(3), 429–438, doi:10.1175/1520-0477(1999)080<0429:MTDUTS>2.0.CO;2.
Hayes, M., M. Svoboda, N. Wall, and M. Widhalm (2011), The Lincoln declaration on drought indices: Universal meteorological drought index recommended, *Bull. Am. Meteorol. Soc.*, *92*(4), 485–488, doi:10.1175/2010BAMS3103.1.
Heim, R. (2002), A review of twentieth-century drought indices used in the United States, *Bull. Am. Meteorol. Soc.*, *83*(8), 1149–1165, doi:10.1175/1520-0477(2002)083<1149:AROTDI>2.3.CO;2.
Heumann, B. W. (2011), Satellite remote sensing of mangrove forests: Recent advances and future opportunities, *Prog. Phys. Geogr.*, *35*(1), 87–108, doi:10.1177/0309133310385371.
Hidalgo, H. G. (2004), Climate precursors of multidecadal drought variability in the western United States, *Water Resour. Res.*, *40*, W12504, doi:10.1029/2004WR003350.
Hielkema, J., S. Prince, and W. Astle (1986), Rainfall and vegetation monitoring in the savanna zone of the Democratic Republic of Sudan using the NOAA advanced very high resolution radiometer, *Int. J. Remote Sens.*, *7*(11), 1499–1513, doi:10.1080/01431168608948950.
Hobbins, M. T., A. Dai, M. L. Roderick, and G. D. Farquhar (2008), Revisiting the parameterization of potential evaporation as a driver of long-term water balance trends, *Geophys. Res. Lett.*, *35*, L12403, doi:10.1029/2008GL033840.
Hoerling, M., and A. Kumar (2003), The perfect ocean for drought, *Science*, *299*(5607), 691–694, doi:10.1126/science.1079053.
Hong, Y., K. Hsu, X. Gao, and S. Sorooshian (2004), Precipitation estimation from remotely sensed imagery using an artificial neural network cloud classification system, *J. Appl. Meteorol. Climatol.*, *43*(12), 1834–1853, doi:10.1175/JAM2173.1.
Hossain, F., and G. Huffman (2008), Investigating error metrics for satellite rainfall data at hydrologically relevant scales, *J. Hydrometeorol.*, *9*(3), 563–575, doi:10.1175/2007JHM925.1.
Houborg, R., M. Rodell, B. Li, R. Reichle, and B. F. Zaitchik (2012), Drought indicators based on model-assimilated Gravity Recovery And Climate Experiment (GRACE) terrestrial water storage observations, *Water Resour. Res.*, *48*, W07525, doi:10.1029/2011WR011291.
Hsu, K., X. Gao, S. Sorooshian, and H. Gupta (1997), Precipitation estimation from remotely sensed information using artificial neural networks, *J. Appl. Meteorol.*, *36*(9), 1176–1190, doi:10.1175/1520-0450(1997)036<1176:PEFRSI>2.0.CO;2.
Huete, A., C. Justice, and W. Van Leeuwen (1999), MODIS Vegetation Index (MOD13), Algorithm Theoretical Basis Document. [Available at http://modis.gsfc.nasa.gov/data/atbd/atbd_mod13.pdf.]
Huete, A., K. Didan, T. Miura, E. P. Rodriguez, X. Gao, and L. G. Ferreira (2002), Overview of the radiometric and biophysical performance of the MODIS vegetation indices, *Remote Sens. Environ.*, *83*(1), 195–213, doi:10.1016/S0034-4257(02)00096-2.
Huete, A. R. (1988), A soil-adjusted vegetation index (SAVI), *Remote Sens. Environ.*, *25*(3), 295–309, doi:10.1016/0034-4257(88)90106-X.
Huete, A. R., K. Didan, Y. E. Shimabukuro, P. Ratana, S. R. Saleska, L. R. Hutyra, W. Yang, R. R. Nemani, and R. Myneni (2006), Amazon rainforests green-up with sunlight in dry season, *Geophys. Res. Lett.*, *33*, L06405, doi:10.1029/2005GL025583.
Huffman, G., R. Adler, D. Bolvin, G. Gu, E. Nelkin, K. Bowman, E. Stocker, and D. Wolff (2007), The TRMM Multi-satellite Precipitation Analysis: Quasi-global, multiyear, combined-sensor precipitation estimates at fine scale, *J. Hydrometeorol.*, *8*(1), 38–55, doi:10.1175/JHM560.1.
Hunt, E. R., and B. N. Rock (1989), Detection of changes in leaf water content using near-and middle-infrared reflectances, *Remote Sens. Environ.*, *30*(1), 43–54, doi:10.1016/0034-4257(89)90046-1.
Huntingford, C., et al. (2013), Simulated resilience of tropical rainforests to CO_2-induced climate change, *Nat. Geosci.*, *6*(4), 268–273, doi:10.1038/ngeo1741.
Idso, S., R. Jackson, P. Pinter, R. Reginato, and J. Hatfield (1981), Normalizing the stress-degree-day parameter for environmental variability, *Agric. Meteorol.*, *24*(1), 45–55, doi:10.1016/0002-1571(81)90032-7.
Jackson, R. D., S. Idso, R. Reginato, and P. Pinter Jr. (1981), Canopy temperature as a crop water stress indicator, *Water Resour. Res.*, *17*(4), 1133–1138, doi:10.1029/WR017i004p01133.
Jackson, T. J. (1993), III. measuring surface soil moisture using passive microwave remote sensing, *Hydrol. Processes*, *7*(2), 139–152, doi:10.1002/hyp.3360070205.
Jackson, T. J. (1997), Soil moisture estimation using special satellite microwave/imager satellite data over a grassland region, *Water Resour. Res.*, *33*(6), 1475–1484, doi:10.1029/97WR00661.
Jackson, T. J., D. Chen, M. Cosh, F. Li, M. Anderson, C. Walthall, P. Doriaswamy, and E. Hunt (2004), Vegetation water content mapping using Landsat data derived normalized difference water index for corn and soybeans, *Remote Sens. Environ.*, *92*(4), 475–482, doi:10.1016/j.rse.2003.10.021.
Jain, S. K., R. Keshri, A. Goswami, A. Sarkar, and A. Chaudhry (2009), Identification of drought-vulnerable areas using NOAA AVHRR data, *Int. J. Remote Sens.*, *30*(10), 2653–2668, doi:10.1080/01431160802555788.
Ji, L., and A. J. Peters (2003), Assessing vegetation response to drought in the northern Great Plains using vegetation and drought indices, *Remote Sens. Environ.*, *87*(1), 85–98, doi:10.1016/S0034-4257(03)00174-3.
Jones, M. O., L. A. Jones, J. S. Kimball, and K. C. McDonald (2011), Satellite passive microwave remote sensing for monitoring global land surface phenology, *Remote Sens. Environ.*, *115*(4), 1102–1114, doi:10.1016/j.rse.2010.12.015.
Joyce, R., and P. A. Arkin (1997), Improved estimates of tropical and subtropical precipitation using the GOES Precipitation Index, *J. Atmos. Oceanic Technol.*, *14*(5), 997–1011, doi:10.1175/1520-0426(1997)014<0997:IEOTAS>2.0.CO;2.

Joyce, R., J. Janowiak, P. Arkin, and P. Xie (2004), CMORPH: A method that produces global precipitation estimates from passive microwave and infrared data at high spatial and temporal resolution, *J. Hydrometeorol.*, *5*(3), 487–503, doi:10.1175/1525-7541(2004)005<0487:CAMTPG>2.0.CO;2.

Justice, C., J. Townshend, E. Vermote, E. Masuoka, R. Wolfe, N. Saleous, D. Roy, and J. Morisette (2002), An overview of MODIS Land data processing and product status, *Remote Sens. Environ.*, *83*(1), 3–15, doi:10.1016/S0034-4257(02)00084-6.

Justice, C. O., et al. (2013), Land and cryosphere products from SUOMI NPP VIIRS: Overview and status, *J. Geophys. Res. Atmos.*, *118*, 9753–9765, doi:10.1002/jgrd.50771.

Kalma, J. D., T. R. McVicar, and M. F. McCabe (2008), Estimating land surface evaporation: A review of methods using remotely sensed surface temperature data, *Surv. Geophys.*, *29*(4-5), 421–469, doi:10.1007/s10712-008-9037-z.

Kao, S., and R. Govindaraju (2010), A copula-based joint deficit index for droughts, *J. Hydrol.*, *380*(1), 121–134, doi:10.1016/j.jhydrol.2009.10.029.

Katiraie-Boroujerdy, P. S., N. Nasrollahi, K. Hsu, and S. Sorooshian (2013), Evaluation of satellite-based precipitation estimation over Iran, *J. Arid Environ.*, *97*, 205–219.

Kim, J., and T. Hogue (2012), Improving spatial soil moisture representation through integration of AMSR-E and MODIS products, *IEEE Trans. Geosci. Remote Sens.*, *50*(2), 446–460.

Krajewski, W. F., M. C. Anderson, W. E. Eichinger, D. Entekhabi, B. K. Hornbuckle, P. R. Houser, G. G. Katul, W. P. Kustas, J. M. Norman, and C. Peters-Lidard (2006), A remote sensing observatory for hydrologic sciences: A genesis for scaling to continental hydrology, *Water Resour. Res.*, *42*, W07301, doi:10.1029/2005WR004435.

Karnieli, A., N. Agam, R. T. Pinker, M. Anderson, M. L. Imhoff, G. G. Gutman, N. Panov, and A. Goldberg (2010), Use of NDVI and land surface temperature for drought assessment: Merits and limitations, *J. Clim.*, *23*(3), 618–633, doi:10.1175/2009JCLI2900.1.

Kelly, R. E., A. T. Chang, L. Tsang, and J. L. Foster (2003), A prototype AMSR-E global snow area and snow depth algorithm, *IEEE Trans. Geosci. Remote Sens.*, *41*(2), 230–242, doi:10.1109/TGRS.2003.809118.

Keyantash, J., and J. Dracup (2004), An aggregate drought index: Assessing drought severity based on fluctuations in the hydrologic cycle and surface water storage, *Water Resour. Res.*, *40*, W09304, doi:10.1029/2003WR002610.

Kidd, C. (2001), Satellite rainfall climatology: A review, *Int. J. Climatol.*, *21*(9), 1041–1066, doi:10.1002/joc.635.

Kiladze, R. I., and A. S. Sochilina (2003), On the new theory of geostationary satellite motion, *Astron. Astrophys. Trans.*, *22*(4-5), 525–528, doi:10.1080/1055679031000111109.

Kogan, F. (1995), Application of vegetation index and brightness temperature for drought detection, *Adv. Space Res.*, *15*(11), 91–100, doi:10.1016/0273-1177(95)00079-T.

Kogan, F., and J. Sullivan (1993), Development of global drought-watch system using NOAA/AVHRR data, *Adv. Space Res.*, *13*(5), 219–222, doi:10.1016/0273-1177(93)90548-P.

Kogan, F. N. (1997), Global drought watch from space, *Bull. Am. Meteorol. Soc.*, *78*(4), 621–636, doi:10.1175/1520-0477(1997)078<0621:GDWFS>2.0.CO;2.

Kogan, F. N. (2001), Operational space technology for global vegetation assessment, *Bull. Am. Meteorol. Soc.*, *82*(9), 1949–1964, doi:10.1175/1520-0477(2001)082<1949:OSTFGV>2.3.CO;2.

Kongoli, C., C. A. Dean, S. R. Helfrich, and R. R. Ferraro (2007), Evaluating the potential of a blended passive microwave-interactive multi-sensor product for improved mapping of snow cover and estimations of snow water equivalent, *Hydrol. Processes*, *21*(12), 1597–1607, doi:10.1002/hyp.6722.

Kongoli, C., P. Romanov, and R. Ferraro (2012), Snow cover monitoring from remote sensing satellites, in *Remote Sensing of Drought: Innovative Monitoring Approaches*, pp. 359–386, CRC Press.

Koster, R. D., M. J. Suarez, A. Ducharne, M. Stieglitz, and P. Kumar (2000), A catchment-based approach to modeling land surface processes in a General Circulation Model: 1. Model structure, *J. Geophys. Res.*, *105*(D20), 24,809–24,822, doi:10.1029/2000JD900327.

Kummerow, C., W. S. Olson, and L. Giglio (1996), A simplified scheme for obtaining precipitation and vertical hydrometeor profiles from passive microwave sensors, *IEEE Trans. Geosci. Remote Sens.*, *34*(5), 1213–1232, doi:10.1109/36.536538.

Kummerow, C., Y. Hong, W. Olson, S. Yang, R. Adler, J. McCollum, R. Ferraro, G. Petty, D.-B. Shin, and T. Wilheit (2001), The evolution of the Goddard profiling algorithm (GPROF) for rainfall estimation from passive microwave sensors, *J. Appl. Meteorol.*, *40*(11), 1801–1820, doi:10.1175/1520-0450(2001)040<1801:TEOTGP>2.0.CO;2.

Kunzi, K. F., S. Patil, and H. Rott (1982), Snow-cover parameters retrieved from NIMBUS-7 scanning multichannel microwave radiometer (SMMR) data, *IEEE Trans. Geosci. Remote Sens.*, *GE-20*(4), 452–467, doi:10.1109/TGRS.1982.350411.

Lambin, E., and D. Ehrlich (1996), The surface temperature-vegetation index space for land cover and land-cover change analysis, *Int. J. Remote Sens.*, *17*(3), 463–487, doi:10.1080/01431169608949021.

Leblanc, M. J., P. Tregoning, G. Ramillien, S. O. Tweed, and A. Fakes (2009), Basin-scale, integrated observations of the early 21st century multiyear drought in southeast Australia, *Water Resour. Res.*, *45*, W04408, doi:10.1029/2008WR007333.

Levizzani, V., P. Bauer, and F. J. Turk (Eds.) (2007), *Measuring Precipitation From Space: EURAINSAT and the Future*, Springer, Dordrecht, Netherlands.

Lewis, S. L., P. M. Brando, O. L. Phillips, G. M. F. van der Heijden, and D. Nepstad (2011), The 2010 Amazon drought, *Science*, *331*(6017), 554, doi:10.1126/science.1200807.

Li, B., M. Rodell, B. F. Zaitchik, R. H. Reichle, R. D. Koster, and T. M. van Dam (2012), Assimilation of GRACE terrestrial water storage into a land surface model: Evaluation and potential value for drought monitoring in western and central Europe, *J. Hydrol.*, *446*, 103–115, doi:10.1016/j.jhydrol.2012.04.035.

Liang, T., X. Zhang, H. Xie, C. Wu, Q. Feng, X. Huang, and Q. Chen (2008), Toward improved daily snow cover mapping with advanced combination of MODIS and AMSR-E measurements, *Remote Sens. Environ.*, *112*(10), 3750–3761, doi:10.1016/j.rse.2008.05.010.

Liu, J. (2004), Investigation of ecosystem drought stress and its impacts on carbon exchange in tropical forests, PhD thesis, Colo. State Univ., Fort Collins.

Liu, W., and F. Kogan (1996), Monitoring regional drought using the Vegetation Condition Index, *Int. J. Remote Sens.*, *17*(14), 2761–2782, doi:10.1080/01431169608949106.

Liu, Y. Y., R. Parinussa, W. Dorigo, R. D. Jeu, W. Wagner, A. I. J. M. van Dijk, M. McCabe, and J. Evans (2011a), Developing an improved soil moisture dataset by blending passive and active microwave satellite-based retrievals, *Hydrol. Earth Syst. Sci.*, *15*(2), 425–436, doi:10.5194/hess-15-425-2011.

Liu, Y. Y., R. A. de Jeu, M. F. McCabe, J. P. Evans, and A. I. J. M. van Dijk (2011b), Global long-term passive microwave satellite-based retrievals of vegetation optical depth, *Geophys. Res. Lett.*, *38*, L18402, doi:10.1029/2011GL048684.

Liu, Y. Y., A. I. J. M. van Dijk, M. F. McCabe, J. P. Evans, and R. A. Jeu (2013a), Global vegetation biomass change (1988–2008) and attribution to environmental and human drivers, *Global Ecol. Biogeogr.*, *22*(6), 692–705, doi:10.1111/geb.12024.

Liu, Y. Y., J. P. Evans, M. F. McCabe, R. A. de Jeu, A. I. J. M. van Dijk, A. J. Dolman, and I. Saizen (2013b), Changing climate and overgrazing are decimating Mongolian steppes, *PloS one*, *8*(2), e57599, doi:10.1371/journal.pone.0057599.
Long, D., B. R. Scanlon, L. Longuevergne, A.-Y. Sun, D. N. Fernando, and S. Himanshu (2013), GRACE satellites monitor large depletion in water storage in response to the 2011 drought in Texas, *Geophys. Res. Lett.*, *40*, 3395–3401, doi:10.1002/grl.50655.
Lu, H., M. R. Raupach, T. R. McVicar, and D. J. Barrett (2003), Decomposition of vegetation cover into woody and herbaceous components using AVHRR NDVI time series, *Remote Sens. Environ.*, *86*(1), 1–18, doi:10.1016/S0034-4257(03)00054-3.
Marengo, J. A., J. Tomasella, L. M. Alves, W. R. Soares, and D. A. Rodriguez (2011), The drought of 2010 in the context of historical droughts in the Amazon region, *Geophys. Res. Lett.*, *38*, L12703, doi:10.1029/2011GL047436.
Margulis, S. A., E. F. Wood, and P. A. Troch (2006), The terrestrial water cycle: Modeling and data assimilation across catchment scales, *J. Hydrometeorol.*, *7*(3), 309–311, doi:10.1175/JHM999.1.
McKee, T., N. Doesken, and J. Kleist (1993), The relationship of drought frequency and duration to time scales, in *Proceedings of the 8th Conference of Applied Climatology, January 1993*, vol. 17, pp. 179–184, Am. Meteorol. Soc., Anaheim, Calif.
McVicar, T. R., and P. B. Bierwirth (2001), Rapidly assessing the 1997 drought in Papua New Guinea using composite AVHRR imagery, *Int. J. Remote Sens.*, *22*(11), 2109–2128, doi:10.1080/01431160120728.
McVicar, T. R., and D. L. Jupp (1998), The current and potential operational uses of remote sensing to aid decisions on drought exceptional circumstances in Australia: A review, *Agric. Syst.*, *57*(3), 399–468, doi:10.1016/S0308-521X(98)00026-2.
McVicar, T. R., and D. L. Jupp (1999), Estimating one-time-of-day meteorological data from standard daily data as inputs to thermal remote sensing based energy balance models, *Agric. For. Meteorol.*, *96*(4), 219–238, doi:10.1016/S0168-1923(99)00052-0.
McVicar, T. R., and D. L. Jupp (2002), Using covariates to spatially interpolate moisture availability in the Murray–Darling Basin: A novel use of remotely sensed data, *Remote Sens. Environ.*, *79*(2), 199–212, doi:10.1016/S0034-4257(01)00273-5.
McVicar, T. R., and C. Körner (2013), On the use of elevation, altitude, and height in the ecological and climatological literature, *Oecologia*, *171*(2), 335–337.
McVicar, T. R., et al. (2012), Global review and synthesis of trends in observed terrestrial near-surface wind speeds: Implications for evaporation, *J. Hydrol.*, *416*, 182–205, doi:10.1016/j.jhydrol.2011.10.024.
Mecikalski, J. R., G. R. Diak, M. C. Anderson, and J. M. Norman (1999), Estimating fluxes on continental scales using remotely sensed data in an atmospheric-land exchange model, *J. Appl. Meteorol.*, *38*(9), 1352–1369, doi:10.1175/1520-0450(1999)038<1352:EFOCSU>2.0.CO;2.
Meesters, A. G., R. A. De Jeu, and M. Owe (2005), Analytical derivation of the vegetation optical depth from the microwave polarization difference index, *IEEE Geosci. Remote Sens. Lett.*, *2*(2), 121–123, doi:10.1109/LGRS.2005.843983.
Mehran, A., and A. AghaKouchak (2014), Capabilities of satellite precipitation datasets to estimate heavy precipitation rates at different temporal accumulations, *Hydrol. Processes*, *28*, 2262–2270, doi:10.1002/hyp.9779.
Meir, P., D. Metcalfe, A. Costa, and R. Fisher (2008), The fate of assimilated carbon during drought: Impacts on respiration in Amazon rainforests, *Philos. Trans. R. Soc. London, Ser. B*, *363*(1498), 1849–1855.
Miao, R., N. Lu, L. Yao, Y. Zhu, J. Wang, and J. Sun (2013), Multi-year comparison of carbon dioxide from satellite data with ground-based FTS measurements (2003–2011), *Remote Sens.*, *5*(7), 3431–3456, doi:10.3390/rs5073431.
Mo, K. C. (2011), Drought onset and recovery over the United States, *J. Geophys. Res.*, *116*, D20106, doi:10.1029/2011JD016168.
Molotch, N. P., and R. C. Bales (2006), Comparison of ground-based and airborne snow surface albedo parameterizations in an alpine watershed: Impact on snowpack mass balance, *Water Resour. Res.*, *42*, W05410, doi:10.1029/2005WR004522.
Molotch, N. P., and S. A. Margulis (2008), Estimating the distribution of snow water equivalent using remotely sensed snow cover data and a spatially distributed snowmelt model: A multi-resolution, multi-sensor comparison, *Adv. Water Res.*, *31*(11), 1503–1514, doi:10.1016/j.advwatres.2008.07.017.
Moran, M., T. Clarke, Y. Inoue, and A. Vidal (1994), Estimating crop water deficit using the relation between surface-air temperature and spectral vegetation index, *Remote Sens. Environ.*, *49*(3), 246–263, doi:10.1016/0034-4257(94)90020-5.
Moran, M. S., C. D. Peters-Lidard, J. M. Watts, and S. McElroy (2004), Estimating soil moisture at the watershed scale with satellite-based radar and land surface models, *Can. J. Remote Sens.*, *30*(5), 805–826, doi:10.5589/m04-043.
Morgan, J. (1989), Satellite remote sensing in meteorology and climatology- status, perspectives and challenges, Deutsche Meteorologen-Tagung ueber Atmosphaere, Ozeane, Kontinente, Kiel, Federal Republic of Germany, May 16-19, 1989, *Ann. Meteorol.*, *26*, 39–43.
Morillas, L., R. Leuning, L. Villagarcía, M. García, P. Serrano-Ortiz, and F. Domingo (2013), Improving evapotranspiration estimates in Mediterranean drylands: The role of soil evaporation, *Water Resour. Res.*, *49*, 6572–6586, doi:10.1002/wrcr.20468.
Mu, Q., F. A. Heinsch, M. Zhao, and S. W. Running (2007), Development of a global evapotranspiration algorithm based on MODIS and global meteorology data, *Remote Sens. Environ.*, *111*(4), 519–536, doi:10.1016/j.rse.2007.04.015.
Mu, Q., L. A. Jones, J. S. Kimball, K. C. McDonald, and S. W. Running (2009), Satellite assessment of land surface evapotranspiration for the pan-Arctic domain, *Water Resour. Res.*, *45*, W09420, doi:10.1029/2008WR007189.
Mu, Q., M. Zhao, and S. W. Running (2011), Improvements to a MODIS global terrestrial evapotranspiration algorithm, *Remote Sens. Environ.*, *115*(8), 1781–1800, doi:10.1016/j.rse.2011.02.019.
Mu, Q., M. Zhao, J. S. Kimball, N. G. McDowell, and S. W. Running (2013), A remotely sensed global terrestrial drought severity index, *Bull. Am. Meteorol. Soc.*, *94*(1), 83–98, doi:10.1175/BAMS-D-11-00213.1.
NASA (1987), *Space-based Remote Sensing of the Earth: A Report to the Congress*, National Aeronautics and Space Administration, Washington, D. C. [Available at http://catalog.hathitrust.org/Record/007403943.]
NASA (1995), *Guidelines and assessment procedures for limiting orbital debris*, vol. 1740. 14, National Aeronautics and Space Administration, Washington, D. C. [Available at http://snebulos.mit.edu/projects/reference/NASA-Generic/NSS_1740.14. pdf.]
NASA (2010), Science plan for NASA's science mission directorate, *Tech. Rep.*, National Aeronautics and Space Administration, Washington, D. C.
Nasrollahi, N., K. Hsu, and S. Sorooshian (2013), An artificial neural network model to reduce false alarms in satellite precipitation products using MODIS and CloudSat observations, *J. Hydrometeorol*, *14*(6), 1872–1883.
Nemani, R., H. Hashimoto, P. Votava, F. Melton, W. Wang, A. Michaelis, L. Mutch, C. Milesi, S. Hiatt, and M. White (2009), Monitoring and forecasting ecosystem dynamics using the Terrestrial Observation and Prediction System (TOPS), *Remote Sens. Environ.*, *113*(7), 1497–1509, doi:10.1016/j.rse.2008.06.017.
Nicholson, S. E., C. J. Tucker, and M. Ba (1998), Desertification, drought, and surface vegetation: An example from the west African Sahel, *Bull. Am. Meteorol. Soc.*, *79*(5), 815–829, doi:10.1175/1520-0477(1998)079<0815:DDASVA>2.0.CO;2.
Njoku, E. G., and D. Entekhabi (1996), Passive microwave remote sensing of soil moisture, *J. Hydrol.*, *184*(1), 101–129, doi:10.1016/0022-1694(95)02970-2.

Njoku, E. G., T. J. Jackson, V. Lakshmi, T. K. Chan, and S. V. Nghiem (2003), Soil moisture retrieval from AMSR-E, *IEEE Trans. Geosci. Remote Sens.*, *41*(2), 215–229, doi:10.1109/TGRS.2002.808243.

Norman, J. M., M. Divakarla, and N. S. Goel (1995), Algorithms for extracting information from remote thermal-IR observations of the Earth's surface, *Remote Sens. Environ.*, *51*(1), 157–168, doi:10.1016/0034-4257(94)00072-U.

Norouzi, H., M. Temimi, W. Rossow, C. Pearl, M. Azarderakhsh, and R. Khanbilvardi (2011), The sensitivity of land emissivity estimates from AMSR-E at C and X bands to surface properties, *Hydrol. Earth Syst. Sci.*, *15*(11), 3577–3589, doi:10.5194/hess-15-3577-2011.

Norouzi, H., W. Rossow, M. Temimi, C. Prigent, M. Azarderakhsh, S. Boukabara, and R. Khanbilvardi (2012), Using microwave brightness temperature diurnal cycle to improve emissivity retrievals over land, *Remote Sens. Environ.*, *123*, 470–482, doi:10.1016/j.rse.2012.04.015.

Norouzi, H., M. Temimi, C. Prigent, J. Turk, R. Khanbilvardi, Y. Tian, F. Furuzawa, and H. Masunaga (2014), Assessment of the consistency among global microwave land surface emissivity products, *Atmos. Meas. Tech. Discuss.*, *7*(9), 9993–10,013, doi:10.5194/amtd-7-9993-2014.

O'grady, A. P., X. Chen, D. Eamus, and L. B. Hutley (2000), Composition, leaf area index and standing biomass of eucalypt open forests near Darwin in the Northern Territory, Australia, *Aust. J. Bot.*, *48*(5), 629–638, doi:10.1071/BT99022.

Otkin, J. A., M. C. Anderson, C. Hain, and M. Svoboda (2014), Examining the relationship between drought development and rapid changes in the Evaporative Stress Index, *J. Hydrometeorol.*, *15*(3), 938–956, doi:10.1175/JHM-D-13-0110.1.

Owe, M., R. de Jeu, and J. Walker (2001), A methodology for surface soil moisture and vegetation optical depth retrieval using the microwave polarization difference index, *IEEE Trans. Geosci. Remote Sens.*, *39*(8), 1643–1654, doi:10.1109/36.942542.

Painter, T. H., F. C. Seidel, A. C. Bryant, S. McKenzie Skiles, and K. Rittger (2013), Imaging spectroscopy of albedo and radiative forcing by light-absorbing impurities in mountain snow, *J. Geophys. Res. Atmos.*, *118*, 9511–9523, doi:10.1002/jgrd.50520.

Palmer, W. (1965), Meteorological drought, Tech. Rep., Weather Bureau Res. Pap. 45, U. S. Dept. of Commerce, 58 pp.

Palmer, W. C. (1968), Keeping track of crop moisture conditions, nationwide: The new crop moisture index, *Weatherwise*, *21*(4), 156–161, doi:10.1080/00431672.1968.9932814.

Palmer, W. C., and A. V. Havens (1958), A graphical technique for determining evapotranspiration by the Thornthwaite method, *Mon. Weather Rev.*, *86*(4), 123–128.

Paridal, B. R., W. B. Collado, R. Borah, M. K. Hazarika, and L. Sarnarakoon (2008), Detecting drought-prone areas of rice agriculture using a MODIS-derived soil moisture index, *GISci. Remote Sens.*, *45*(1), 109–129, doi:10.2747/1548-1603.45.1.109.

Park, J.-S., K.-T. Kim, and Y.-S. Choi (2008), Application of vegetation condition index and standardized vegetation index for assessment of spring drought in South Korea, in *Geoscience and Remote Sensing Symposium, 2008. IGARSS 2008. IEEE International*, vol. 3, pp. 774–777, IEEE, Boston, Mass.

Patel, N., B. Parida, V. Venus, S. Saha, and V. Dadhwal (2012), Analysis of agricultural drought using Vegetation Temperature Condition Index (VTCI) from TERRA/MODIS satellite data, *Environ. Monit. Assess.*, *184*(12), 7153–7163.

Payero, J., C. Neale, and J. Wright (2004), Comparison of eleven vegetation indices for estimating plant height of alfalfa and grass, *Appl. Eng. Agric.*, *20*(3), 385–393.

Perry, C. R., and L. F. Lautenschlager (1984), Functional equivalence of spectral vegetation indices, *Remote Sens. Environ.*, *14*(1), 169–182.

Peters, A. J., E. A. Walter-Shea, L. Ji, A. Vina, M. Hayes, and M. D. Svoboda (2002), Drought monitoring with NDVI-based standardized vegetation index, *Photogramm. Eng. Remote Sens.*, *68*(1), 71–75.

Peters-Lidard, C. D., D. M. Mocko, M. Garcia, J. A. Santanello, M. A. Tischler, M. S. Moran, and Y. Wu (2008), Role of precipitation uncertainty in the estimation of hydrologic soil properties using remotely sensed soil moisture in a semiarid environment, *Water Resour. Res.*, *44*, W05S18, doi:10.1029/2007WR005884.

Phillips, O. L., et al. (1998), Changes in the carbon balance of tropical forests: Evidence from long-term plots, *Science*, *282*(5388), 439–442.

Piechota, T. C., and J. A. Dracup (1996), Drought and regional hydrologic variation in the United States: Associations with the El Niño-Southern Oscillation, *Water Resour. Res.*, *32*(5), 1359–1373.

Pinker, R. T., D. Sun, M.-P. Hung, C. Li, and J. B. Basara (2009), Evaluation of satellite estimates of land surface temperature from GOES over the United States, *J. Appl. Meteorol. Climatol.*, *48*(1), 167–180.

Pinzon, J. E., and C. J. Tucker (2014), A non-stationary 1981-2012 AVHRR NDVI3g time series, *Remote Sens.*, *6*(8), 6929–6960, doi:10.3390/rs6086929.

Pook, E. W. (1985), Canopy dynamics of Eucalyptus maculata Hook. III. Effects of drought, *Aust. J. Bot.*, *33*(1), 65–79.

Pook, E. W. (1986), Canopy dynamics of Eucalyptus-maculata Hook. 4. Contrasting responses to two severe droughts, *Aust. J. Bot.*, *34*(1), 1–14.

Pook, E. W., A. M. Gill, and P. H. R. Moore (1997), Long-term variation of litter fall, canopy leaf area and flowering in a Eucalyptus maculata forest on the south coast of New South Wales, *Aust. J. Bot.*, *45*(5), 737–755, doi:10.1071/BT95063.

Poulter, B., et al. (2014), Contribution of semi-arid ecosystems to interannual variability of the global carbon cycle, *Nature*, *509*(7502), 600–603.

Price, J. C. (1982), Estimation of regional scale evapotranspiration through analysis of satellite thermal-infrared data, *IEEE Trans. Geosci. Remote Sens.*, *GE-20*(3), 286–292.

Prince, S. D., D. Colstoun, E. Brown, and L. Kravitz (1998), Evidence from rain-use efficiencies does not indicate extensive Sahelian desertification, *Global Change Biol.*, *4*(4), 359–374.

Qin, Q., C. Jin, N. Zhang, and X. Yang (2010), An two-dimensional spectral space based model for drought monitoring and its re-examination, in *Geoscience and Remote Sensing Symposium (IGARSS), 2010*, pp. 3869–3872, IEEE.

Quiring, S. M., and S. Ganesh (2010), Evaluating the utility of the Vegetation Condition Index (VCI) for monitoring meteorological drought in Texas, *Agric. For. Meteorol.*, *150*(3), 330–339.

Rajsekhar, D., V. P. Singh, and A. K. Mishra (2014), Multivariate drought index: An information theory based approach for integrated drought assessment, *J. Hydrol.*, *526*, 164–182, doi:10.1016/j.jhydrol.2014.11.031.

Rasmusson, E. M., et al. (1983), Meteorological aspects of the El Niño-Southern Oscillation, *Science*, *222*(4629), 1195–1202.

Reichle, R. H., R. D. Koster, J. Dong, and A. A. Berg (2004), Global soil moisture from satellite observations, land surface models, and ground data: Implications for data assimilation, *J. Hydrometeorol.*, *5*(3), 430–442.

Reichle, R. H., R. D. Koster, G. J. De Lannoy, B. A. Forman, Q. Liu, S. P. Mahanama, and A. Touré (2011), Assessment and enhancement of MERRA land surface hydrology estimates, *J. Clim.*, *24*(24), 6322–6338.

Rhee, J., J. Im, and G. J. Carbone (2010), Monitoring agricultural drought for arid and humid regions using multi-sensor remote sensing data, *Remote Sens. Environ.*, *114*(12), 2875–2887.

Richard, Y., and I. Poccard (1998), A statistical study of NDVI sensitivity to seasonal and interannual rainfall variations in Southern Africa, *Int. J. Remote Sens.*, *19*(15), 2907–2920.

Rodell, M. (2012), Satellite gravimetry applied to drought monitoring, in *Remote Sensing of Drought: Innovative Monitoring Approaches*, pp. 261–277, CRC Press.
Rodell, M., and J. Famiglietti (2002), The potential for satellite-based monitoring of groundwater storage changes using GRACE: The high plains aquifer, central US, *J. Hydrol.*, *263*(1), 245–256.
Rodell, M., J. Chen, H. Kato, J. S. Famiglietti, J. Nigro, and C. R. Wilson (2007), Estimating groundwater storage changes in the Mississippi River Basin (USA) using GRACE, *Hydrogeol. J.*, *15*(1), 159–166.
Roderick, M. L., I. R. Noble, and S. W. Cridland (1999), Estimating woody and herbaceous vegetation cover from time series satellite observations, *Global Ecol. Biogeogr.*, *8*(6), 501–508.
Romanov, P., G. Gutman, and I. Csiszar (2000), Automated monitoring of snow cover over North America with multispectral satellite data, *J. Appl. Meteorol.*, *39*(11), 1866–1880.
Rott, H., et al. (2010), Cold regions hydrology high-resolution observatory for snow and cold land processes, *Proc. IEEE*, *98*(5), 752–765.
Rouse, J., R. Haas, J. Schell, D. Deering, and J. Harlan (1974), *Monitoring the Vernal Advancement and Retrogradation (Greenwave Effect) of Natural Vegetation*, 362 pp., Texas A & M Univ., Remote Sens. Cent., College Station, Tex.
Running, S. W., R. R. Nemani, D. L. Peterson, L. E. Band, D. F. Potts, L. L. Pierce, and M. A. Spanner (1989), Mapping regional forest evapotranspiration and photosynthesis by coupling satellite data with ecosystem simulation, *Ecology*, *70*(4), 1090–1101.
Running, S. W., R. R. Nemani, F. A. Heinsch, M. Zhao, M. Reeves, and H. Hashimoto (2004), A continuous satellite-derived measure of global terrestrial primary production, *Bioscience*, *54*(6), 547–560.
Saleska, S. R., K. Didan, A. R. Huete, and H. R. da Rocha (2007), Amazon forests green-up during 2005 drought, *Science*, *318*(5850), 612, doi:10.1126/science.1146663.
Santos, J. F., I. Pulido-Calvo, and M. M. Portela (2010), Spatial and temporal variability of droughts in Portugal, *Water Resour. Res.*, *46*, W03503, doi:10.1029/2009WR008071.
Schanda, E., C. Matzler, and K. Kunzi (1983), Microwave remote sensing of snow cover, *Int. J. Remote Sens.*, *4*(1), 149–158.
Seiler, R., F. Kogan, and J. Sullivan (1998), AVHRR-based vegetation and temperature condition indices for drought detection in Argentina, *Adv. Space Res.*, *21*(3), 481–484.
Sellars, S., P. Nguyen, W. Chu, X. Gao, K.-l. Hsu, and S. Sorooshian (2013), Computational Earth science: Big data transformed into insight, *EOS Trans. AGU*, *94*(32), 277–278.
Senay, G. B. (2008), Modeling landscape evapotranspiration by integrating land surface phenology and a water balance algorithm, *Algorithms*, *1*(2), 52–68.
Senay, G. B., M. Budde, J. P. Verdin, and A. M. Melesse (2007), A coupled remote sensing and simplified surface energy balance approach to estimate actual evapotranspiration from irrigated fields, *Sensors*, *7*(6), 979–1000.
Senay, G. B., S. Bohms, and J. P. Verdin (2012), Remote sensing of evapotranspiration for operational drought monitoring using principles of water and energy balance, in *Remote Sensing of Drought: Innovative Monitoring Approaches*, edited by B. D. Wardlow, M. C. Anderson, and J. P. Verdin, pp. 123–144, CRC Press.
Sheffield, J., G. Goteti, F. Wen, and E. Wood (2004), A simulated soil moisture based drought analysis for the United States, *J. Geophys. Res.*, *109*, D24108, doi:10.1029/2004JD005182.
Sheffield, J., G. Goteti, and E. Wood (2006), Development of a 50-yr, high resolution global dataset of meteorological forcings for land surface modeling, *J. Clim.*, *13*, 3088–3111.
Sheffield, J., E. Wood, and M. Roderick (2012), Little change in global drought over the past 60 years, *Nature*, *491*(7424), 435–438.
Shen, H. W., and G. Q. Tabios (1996), *Modeling of Precipitation-Based Drought Characteristics Over California*, Centers for Water and Wildland Resources, Series: California Water Resources Center, 204. [Available at http://library.wur.nl/WebQuery/clc/929134.]
Shi, J., T. Jackson, J. Tao, J. Du, R. Bindlish, L. Lu, and K. Chen (2008), Microwave vegetation indices for short vegetation covers from satellite passive microwave sensor AMSR-E, *Remote Sens. Environ.*, *112*(12), 4285–4300.
Silleos, N. G., T. K. Alexandridis, I. Z. Gitas, and K. Perakis (2006), Vegetation indices: Advances made in biomass estimation and vegetation monitoring in the last 30 years, *Geocarto Int.*, *21*(4), 21–28.
Simpson, J., J. Stitt, and M. Sienko (1998), Improved estimates of the areal extent of snow cover from AVHRR data, *J. Hydrol.*, *204*(1), 1–23.
Singh, R. P., S. Roy, and F. Kogan (2003), Vegetation and temperature condition indices from NOAA AVHRR data for drought monitoring over India, *Int. J. Remote Sens.*, *24*(22), 4393–4402.
Smith, P., et al. (2010), European-wide simulations of croplands using an improved terrestrial biosphere model: Phenology and productivity, *J. Geophys. Res.*, *115*, G01014, doi:10.1029/2008JG000800.
Son, N., C. Chen, C. Chen, L. Chang, and V. Minh (2012), Monitoring agricultural drought in the lower Mekong basin using MODIS NDVI and land surface temperature data, *Int. J. Appl. Earth Obs. Geoinf.*, *18*, 417–427.
Sorooshian, S., K. Hsu, X. Gao, H. Gupta, B. Imam, and D. Braithwaite (2000), Evolution of the PERSIANN system satellite-based estimates of tropical rainfall, *Bull. Am. Meteorol. Soc.*, *81*(9), 2035–2046.
Sorooshian, S., et al. (2011), Advanced concepts on remote sensing of precipitation at multiple scales, *Bull. Am. Meteorol. Soc.*, *92*(10), 1353–1357.
Specht, R. (1972), Water use by perennial evergreen plant communities in Australia and Papua New Guinea, *Aust. J. Bot.*, *20*(3), 273–299, doi:10.1071/BT9720273.
Su, H., M. McCabe, E. Wood, Z. Su, and J. Prueger (2005), Modeling evapotranspiration during SMACEX: Comparing two approaches for local-and regional-scale prediction, *J. Hydrometeorol.*, *6*(6), 910–922.
Sun, D., and M. Kafatos (2007), Note on the NDVI-LST relationship and the use of temperature-related drought indices over North America, *Geophys. Res. Lett.*, *34*, L24406, doi:10.1029/2007GL031485.
Svoboda, M., et al. (2002), The drought monitor, *Bull. Am. Meteorol. Soc.*, *83*(8), 1181–1190.
Swain, S., B. D. Wardlow, S. Narumalani, T. Tadesse, and K. Callahan (2011), Assessment of vegetation response to drought in Nebraska using TERRA-MODIS land surface temperature and normalized difference vegetation index, *GISci. Remote Sens.*, *48*(3), 432–455.
Tadesse, T., J. Brown, and M. Hayes (2005), A new approach for predicting drought-related vegetation stress: Integrating satellite, climate, and biophysical data over the US central plains, *ISPRS J. Photogramm. Remote Sens.*, *59*(4), 244–253.
Takada, M., Y. Mishima, and S. Natsume (2009), Estimation of surface soil properties in peatland using ALOS/PALSAR, *Landscape Ecol. Eng.*, *5*(1), 45–58.
Tedesco, M., and E. J. Kim (2006), Retrieval of dry-snow parameters from microwave radiometric data using a dense-medium model and genetic algorithms, *IEEE Trans. Geosci. Remote Sens.*, *44*(8), 2143–2151.
Thiam, A. K. (1998), *Geographic Information Systems and Remote Sensing Methods for Assessing and Monitoring Land Degradation in the Sahel Region: The Case of Southern Mauritania*, Clark Univ., Worcester, Mass. [Available at http://adsabs.harvard.edu/abs/1998PhDT.....94T.]

Thomas, A. C., J. T. Reager, J. S. Famiglietti, and M. Rodell (2014), A GRACE-based water storage deficit approach for hydrological drought characterization, *Geophys. Res. Lett.*, *41*, 1537–1545, doi:10.1002/2014GL059323.
Tian, Y., C. Peters-Lidard, J. Eylander, R. Joyce, G. Huffman, R. Adler, K. Hsu, F. Turk, M. Garcia, and J. Zeng (2009), Component analysis of errors in satellite-based precipitation estimates, *J. Geophys. Res.*, *114*, D24101, doi:10.1029/2009JD011949.
Tsakiris, G., and H. Vangelis (2005), Establishing a drought index incorporating evapotranspiration, *European Water*, *9*(10), 3–11.
Tsakiris, G., D. Pangalou, and H. Vangelis (2007), Regional drought assessment based on the Reconnaissance Drought Index (RDI), *Water Resour. Manage.*, *21*(5), 821–833.
Tucker, C. J. (1979), Red and photographic infrared linear combinations for monitoring vegetation, *Remote Sens. Environ.*, *8*(2), 127–150.
Tucker, C. J., and B. J. Choudhury (1987), Satellite remote sensing of drought conditions, *Remote Sens. Environ.*, *23*(2), 243–251.
Tucker, C. J., J. E. Pinzon, M. E. Brown, D. A. Slayback, E. W. Pak, R. Mahoney, E. F. Vermote, and N. El Saleous (2005), An extended AVHRR 8-km NDVI dataset compatible with MODIS and SPOT vegetation NDVI data, *Int. J. Remote Sens.*, *26*(20), 4485–4498.
Turk, F. J., G. D. Rohaly, J. Hawkins, E. A. Smith, F. S. Marzano, A. Mugnai, and V. Levizzani (1999), Meteorological applications of precipitation estimation from combined SSM/I, TRMM and infrared geostationary satellite data, in *Microwave Radiometry and Remote Sensing of the Earth's Surface and Atmosphere*, edited by P. Pampaloni and S. Paloscia, pp. 353–363, VSP Int. Sci. Publisher, Utrecht, Netherlands.
UNESCO (1979), Map of the world distribution of arid regions, *Tech. Rep.*, The United Nations Educational, Scientific and Cultural Organization (UNESCO), Paris, France.
Unganai, L. S., and F. N. Kogan (1998), Drought monitoring and corn yield estimation in southern Africa from AVHRR data, *Remote Sens. Environ.*, *63*(3), 219–232.
Van der Molen, M., et al. (2011), Drought and ecosystem carbon cycling, *Agric. For. Meteorol.*, *151*(7), 765–773.
van Dijk, A. I. J. M., L. Renzullo, and M. Rodell (2011), Use of Gravity Recovery and Climate Experiment terrestrial water storage retrievals to evaluate model estimates by the Australian water resources assessment system, *Water Resour. Res.*, *47*, W11524, doi:10.1029/2011WR010714.
van Dijk, A. I. J. M., H. E. Beck, R. S. Crosbie, R. A. Jeu, Y. Y. Liu, G. M. Podger, B. Timbal, and N. R. Viney (2013), The millennium drought in southeast Australia (2001–2009): Natural and human causes and implications for water resources, ecosystems, economy, and society, *Water Resour. Res.*, *49*, 1040–1057, doi:10.1002/wrcr.20123.
Van Niel, T., T. R. McVicar, H. Fang, and S. Liang (2003), Calculating environmental moisture for per-field discrimination of rice crops, *Int. J. Remote Sens.*, *24*(4), 885–890.
Vargas, M., T. Miura, N. Shabanov, and A. Kato (2013), An initial assessment of SUOMI NPP VIIRS vegetation index EDR, *J. Geophys. Res. Atmos.*, *118*, 12–301, doi:10.1002/2013JD020439.
Vetter, M., et al. (2008), Analyzing the causes and spatial pattern of the European 2003 carbon flux anomaly using seven models, *Biogeosciences*, *5*(2), 561–583.
Vicente-Serrano, S. M., S. Beguera, J. Lorenzo-Lacruz, J. J. Camarero, J. I. Lpez-Moreno, C. Azorin-Molina, J. Revuelto, E. Morn-Tejeda, and A. Sanchez-Lorenzo (2012), Performance of drought indices for ecological, agricultural, and hydrological applications, *Earth Interact.*, *16*(10), 1–27, doi:10.1175/2012EI000434.1.
Wagner, W., J. Noll, M. Borgeaud, and H. Rott (1999), Monitoring soil moisture over the Canadian prairies with the ERS scatterometer, *IEEE Trans. Geosci. Remote Sens.*, *37*(1), 206–216.
Wagner, W., W. Dorigo, R. de Jeu, D. Fernandez, J. Benveniste, E. Haas, and M. Ertl (2012), Fusion of active and passive microwave observations to create an essential climate variable data record on soil moisture, *XXII ISPRS Congress, Melbourne, Australia*. [Available at http://www.isprs-ann-photogramm-remote-sens-spatial-inf-sci.net/I-7/315/2012/ isprsannals-I-7-315-2012.pdf.]
Wan, Z., P. Wang, and X. Li (2004), Using MODIS land surface temperature and normalized difference vegetation index products for monitoring drought in the southern Great Plains, USA, *Int. J. Remote Sens.*, *25*(1), 61–72.
Wang, A., T. J. Bohn, S. P. Mahanama, R. D. Koster, and D. P. Lettenmaier (2009), Multimodel ensemble reconstruction of drought over the continental United States, *J. Clim.*, *22*(10), 2694–2712.
Wang, J., K. Price, and P. Rich (2001), Spatial patterns of NDVI in response to precipitation and temperature in the central Great Plains, *Int. J. Remote Sens.*, *22*(18), 3827–3844.
Wang, K., and R. E. Dickinson (2012), A review of global terrestrial evapotranspiration: Observation, modeling, climatology, and climatic variability, *Rev. Geophys.*, *50*, RG2005, doi:10.1029/2011RG000373.
Wang, L., and J. J. Qu (2007), NMDI: A Normalized Multi-band Drought Index for monitoring soil and vegetation moisture with satellite remote sensing, *Geophys. Res. Lett.*, *34*, L20405, doi:10.1029/2007GL031021.
Wang, L., and J. J. Qu (2009), Satellite remote sensing applications for surface soil moisture monitoring: A review, *Front. Earth Sci. Chin.*, *3*(2), 237–247.
Wang, L., J. J. Qu, X. Hao, and Q. Zhu (2008), Sensitivity studies of the moisture effects on MODIS SWIR reflectance and vegetation water indices, *Int. J. Remote Sens.*, *29*(24), 7065–7075.
Wang, Y., R. Law, and B. Pak (2010), A global model of carbon, nitrogen and phosphorus cycles for the terrestrial biosphere, *Biogeosciences*, *7*(7), 2261–2282.
Wardlow, B., M. C. Anderson, and J. Verdin (2012), *Remote Sensing of Drought: Innovative Monitoring Approaches*, pp. 484, CRC Press.
Wegren, S. K. (2011), Food security and Russia's 2010 drought, *Eurasian Geogr. Econ.*, *52*(1), 140–156.
Welsch, C., H. Swenson, S. A. Cota, F. DeLuccia, J. M. Haas, C. Schueler, R. M. Durham, J. E. Clement, and P. E. Ardanuy (2001), VIIRS (visible infrared imager radiometer suite): A next-generation operational environmental sensor for NPOESS, in *Geoscience and Remote Sensing Symposium, 2001. IGARSS'01*, vol. 3, pp. 1020–1022, IEEE, Sydney, NSW.
Werick, W., G. Willeke, N. Guttman, J. Hosking, and J. Wallis (1994), National drought atlas developed, *EOS Trans. AGU*, *75*(8), 89.
Wiegand, C., A. Richardson, D. Escobar, and A. Gerbermann (1991), Vegetation indices in crop assessments, *Remote Sens. Environ.*, *35*(2), 105–119.
Wiesnet, D. (1981), Winter snow drought, *EOS Trans. AGU*, *62*(14), 137–137.
Wilhite, D. A. (2005), *Drought and Water Crises: Science, Technology, and Management Issues*, pp. 432, vol. 86, CRC Press.
Wilson, W. J., S. H. Yueh, S. J. Dinardo, S. L. Chazanoff, A. Kitiyakara, F. K. Li, and Y. Rahmat-Samii (2001), Passive active L-and S-band (pals) microwave sensor for ocean salinity and soil moisture measurements, *IEEE Trans. Geosci. Remote Sens.*, *39*(5), 1039–1048.
Wiscombe, W. J., and S. G. Warren (1980), A model for the spectral albedo of snow. I: Pure snow, *J. Atmos. Sci.*, *37*(12), 2712–2733.
WMO (2009), *Inter-Regional Workshop on Indices and Early Warning Systems for Drought*, World Meteorological Organization, Lincoln, Nebraska, 8-11 December 2009.
Woodwell, G. M., and R. H. Whittaker (1968), Primary production in terrestrial ecosystems, *Am. Zool.*, *8*(1), 19–30.
Yang, Y., and S. Shang (2013), A hybrid dual-source scheme and trapezoid framework-based evapotranspiration model (HTEM) using satellite images: Algorithm and model test, *J. Geophys. Res. Atmos.*, *118*, 2284–2300, doi:10.1002/jgrd.50259.

Yang, Y., D. Long, H. Guan, B. R. Scanlon, C. T. Simmons, L. Jiang, and X. Xu (2014), GRACE satellite observed hydrological controls on interannual and seasonal variability in surface greenness over mainland Australia, *J. Geophys. Res. Biogeosci.*, *119*, 2245–2260, doi:10.1002/2014JG002670.

Yao, Y., S. Liang, Q. Qin, and K. Wang (2010), Monitoring drought over the Conterminous United States using MODIS and NCEP reanalysis-2 data, *J. Appl. Meteorol. Climatol.*, *49*(8), 1665–1680.

Yao, Y., S. Liang, Q. Qin, K. Wang, and S. Zhao (2011), Monitoring global land surface drought based on a hybrid evapotranspiration model, *Int. J. Appl. Earth Obs. Geoinf.*, *13*(3), 447–457.

Yebra, M., A. I. J. M. van Dijk, R. Leuning, A. Huete, and J. P. Guerschman (2013), Evaluation of optical remote sensing to estimate actual evapotranspiration and canopy conductance, *Remote Sens. Environ.*, *129*, 250–261.

Yin, D., M. L. Roderick, G. Leech, F. Sun, and Y. Haung (2014), The contribution of reduction in evaporative cooling to higher surface air temperatures during drought, *Geophys. Res. Lett.*, *41*, 7891–7897, doi:10.1002/2014GL062039.

Yirdaw, S. Z., K. R. Snelgrove, and C. O. Agboma (2008), GRACE satellite observations of terrestrial moisture changes for drought characterization in the Canadian prairie, *J. Hydrol.*, *356*(1), 84–92.

Yuan, W., et al. (2014), Multiyear precipitation reduction strongly decreases carbon uptake over northern China, *J. Geophys. Res. Biogeosci.*, *119*, 881–896, doi:10.1002/2014JG002608.

Zaitchik, B. F., M. Rodell, and R. H. Reichle (2008), Assimilation of GRACE terrestrial water storage data into a land surface model: Results for the Mississippi River Basin, *J. Hydrometeorol.*, *9*(3), 535–548.

Zhang, A., and G. Jia (2013), Monitoring meteorological drought in semiarid regions using multi-sensor microwave remote sensing data, *Remote Sens. Environ.*, *134*(12–13), 12–23.

Zhang, N., Y. Hong, Q. Qin, and L. Liu (2013), VSDI: A Visible and Shortwave infrared Drought Index for monitoring soil and vegetation moisture based on optical remote sensing, *Int. J. Remote Sens.*, *34*(13), 4585–4609.